water

MDPI

Article

# Change in the Extent of Glaciers and Glacier Runoff in the Chinese Sector of the Ile River Basin between 1962 and 2012

**Larissa Kogutenko [1,2,*], Igor Severskiy [3], Maria Shahgedanova [4] and Bigzhang Lin [1]**

[1] Department of Athmospheric Science, Nanjing University of Information Science and Technology, Nanjing 210044, China
[2] UNESCO Chair on Integrated Water Recourses Management, Kazakh-German University, Almaty 050010, Kazakhstan
[3] Department of Glaciology, Institute of Geography, Almaty 050010, Kazakhstan
[4] School of Archaeology, Geography and Environmental Science (SAGES), The University of Reading, Reading RG6 6AB, UK
* Correspondence: kogutenko_larissa@mail.ru

Received: 30 June 2019; Accepted: 7 August 2019; Published: 12 August 2019


**Abstract:** Change in glacier area in the Kuksu and Kunes river basins, which are tributaries to the internationally important Ile River, were assessed at two different time steps between 1962/63, 1990/93, and 2010/12. Overall, glaciers lost 191.3 ± 16.8 km$^2$ or 36.9 ± 6.5% of the initial area. Glacier wastage intensified in the latter period: While in 1962/63–1990/93 glaciers were losing 0.5% a$^{-1}$, in 1990/93–2010/12, they were losing 1.2% a$^{-1}$. Streamflow of the Ile River and its tributaries do not exhibit statistically significant change during the vegetative period between May and September. Positive trends were observed in the Ile flow in autumn, winter, and early spring. By contrast, the calculation of the total runoff from the glacier surface (including snow and ice melt) using temperature-index method and runoff forming due to melting of multiyear ice estimated from changes in glacier volume at different time steps between the 1960s and 2010s, showed that their absolute values and their contribution to total river runoff declined since the 1980s. This change is attributed to a strong reduction in glacier area.

**Keywords:** glacier changes; Tien Shan mountains; glacier runoff

## 1. Introduction

Water security is one of the major problems in Central Asia. Most rivers start in the glacierized Tien Shan Mountains and have snow and glacier nourishment [1,2]. The rapidly growing water consumption, caused by population growth, expansion of agriculture, industrial development, and poor water management, can be potentially aggravated by the decline in snow resources in the mountain runoff formation zone and glacier degradation, which occurs across the mountains of Central Asia in response to the observed climatic warming [3]. A strong reduction in area and volume of the Tien Shan glaciers since the mid-20th century has been reported in a number of studies [1,4–16].

Between the 1950s and the early 1970s, glaciers in Tien Shan remained mostly in a stable condition. An acceleration of the glacier degradation across most of the Tien Shan occurred at the beginning of the 1970s. This is confirmed by negative mean values of annual mass balance which, in 1969–1994, were −570 mm w.e. at the Abramov Glacier, −550 mm w.e. at the Karabatkak Glacier, and −310 at the Golubin Glacier [17], and the continuing reduction in the extent of glaciers approximately since 1973 [6,9–11,18–24]. Glaciers located in the outer ranges experienced stronger retreat [16] while glaciers locate in the intermountain basins exhibited slower retreat [25] due to the higher absolute elevations

and higher elevation of the equilibrium line altitude (ELA). Glacier retreat intensified further from the beginning of the 20th century, ranging from 0.8–1.1% $a^{-1}$ in the outer ranges [11,16,26] to 0.30–0.35% $a^{-1}$ in the Eastern and Inner Tien Shan [6,25,27].

At present, despite the observed glacier recession, there is no evidence for a decline in river discharge in the natural glacierized catchments [20,28–31]. However, further glacier degradation is projected for the region, in line with the projected climatic warming, eventually leading to a decline in discharge, especially in the summer months [32–34]. In the glacierized catchments, streamflow draws water from liquid precipitation and from melting of seasonal snow, glacier, and ground ice. Changes in the contribution of the melting glacier ice can be masked by variability in precipitation [2]. It is, therefore, important to assess a relative contribution of the melting glacier ice to the streamflow.

Most of the major rivers of Central Asia are transboundary. Assessments of water resources, including changes in the extent of glaciers and their contribution to the streamflow are important for policy-makers at national and international levels [35]. The Ile River is one of the main transboundary rivers in Central Asia, whose glacierized catchment is shared by China and Kazakhstan. More than 70% of runoff of the Ile River is formed in China. The Ile River flows into Lake Balkhash, located in south-eastern Kazakhstan, contributing about 80% of the total river inflow into the lake. The Balkhash is one of the largest endorheic lakes in Central Asia and sustainability of the Ile's runoff is crucial for maintaining the hydrological and ecological regimes of the lake [36,37], as well as for the economy and ecosystems in this vast region [20].

Although two glacier inventories were conducted in the Chinese sector of the Ile basin, our knowledge of glacier change in this region is less detailed than in other regions of Central Asia, where multiple inventories have been conducted with the time step of 10–20 years [2]. The First Chinese Glacier Inventory (FCGI) was derived from the aerial photography obtained in 1959–1963 [38]. The Second Chinese Glacier Inventory (SCGI) was based on the satellite imagery from 2007–2009 [39]. Between these periods, glaciers of the Upper Ile glacier system lost 24.2 ± 8.8% of their area [8,40]. However, there was no evaluation of changes in the rates of glacier area and volume reduction at different time steps since the 1960s, or contribution of glacial melt water into the streamflow.

This paper has three objectives: (i) Building on previous research, to provide an assessment of glacier change at different time steps between the 1960s and 2012/13 in the three sub-basins (Kunes, Kuksu, and Qiedeke) of the Chinese sector of the Ile River Basin (C-IRB); (ii) examine temporal trends in seasonal discharge of the Ile and its tributaries; and (iii) assess glacier runoff in the study area and evaluate changes in glacier component of the Ile River runoff.

Glacier runoff is defined in different ways in Central Asia, meaning either total runoff from glacier surface or runoff generated by melting ice [2]. We use terms 'total glacier runoff' or 'runoff from glacier/glacierized surfaces' denoting runoff generated by melting snow on the glacier surface, firn, and ice. The term 'glacier ice runoff' refers to runoff generated specifically by melting glacier ice.

## 2. Study Area

The transboundary Ile basin accommodates the glacier systems of the Northern Tien Shan and the Jetisu (also known as Jungar or Dzhungarskiy) Alatau Mountains (Figure 1). The vast majority of glaciers are located in the C-IRB, which has a total area 61,640 $km^2$, 3% of which is glacierized. In 1963, there were 2373 glaciers with a total area and ice volume of 2022.66 $km^2$ and 142.18 $km^3$, respectively, distributed between the five sub-basins: The Khorgos, Kax, Kunes, Kuksu, and Tekes [8]. Of these sub-basins, the Kuksu and Tekes are most the heavily glacierized and accommodate over 70% of the total glacier area and 76% of the glacier ice volume.

According to [41], the mean annual runoff of the Ile is 17.0 $km^3$ (as measured at the Yamadu station) and the mean depth of runoff is 275.8 mm. Of this, Kazakhstan receives 11.7 $km^3$ while 0.00096 $km^3$ is delivered from Kazakhstan to China by the Tekes, which is a tributary to the Ile. It was previously estimated that glaciers supply about 16.5% of the total surface runoff [8].

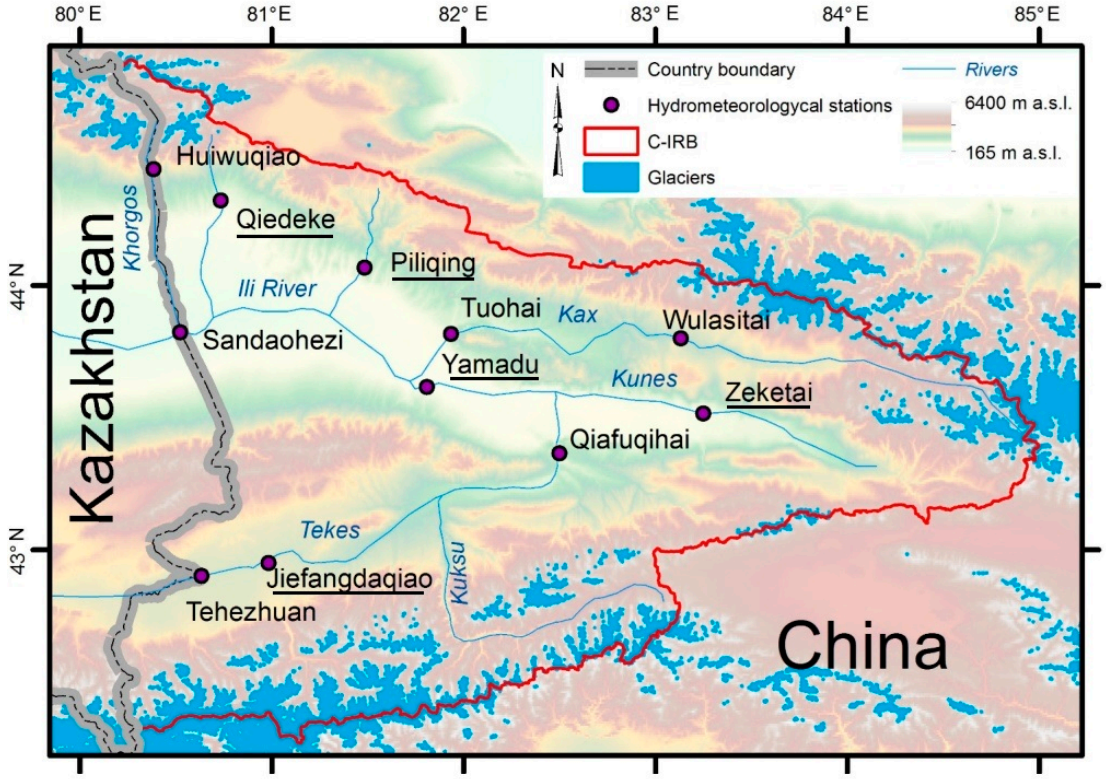


**Figure 1.** Study area. Stations used for trend analysis are underlined.

*Climate*

The main features of climate of the Tien Shan Mountains (including the Eastern Tien Shan), which can be described as temperate continental, were analyzed in [42]. The absolute elevations exceed 6000 m a.s.l. in the region, and both temperature and precipitation regimes depend on and vary with elevation. Temperature inversions are an important feature of the winter climate (November to March) in the lower mountains below approximately 2000 m a.s.l. [42,43]. In the warm period (May to August), mean air temperature at the equilibrium line altitude (ELA) varies between −2.5 and +4.2 °C [8].

The highest annual precipitation (>800 mm) is observed in the Kax and Kunes river basins [41]. In other regions of the C-IRB, annual precipitation decreases to 200 mm, and the same annual totals are observed in the Ile Depression near the Kazakhstan border (Figure 2). Mean elevation of the snow line increases from 3710 m in the Kunes River basin to 3840 m in the Kuksu basin, in line with decreasing precipitation.

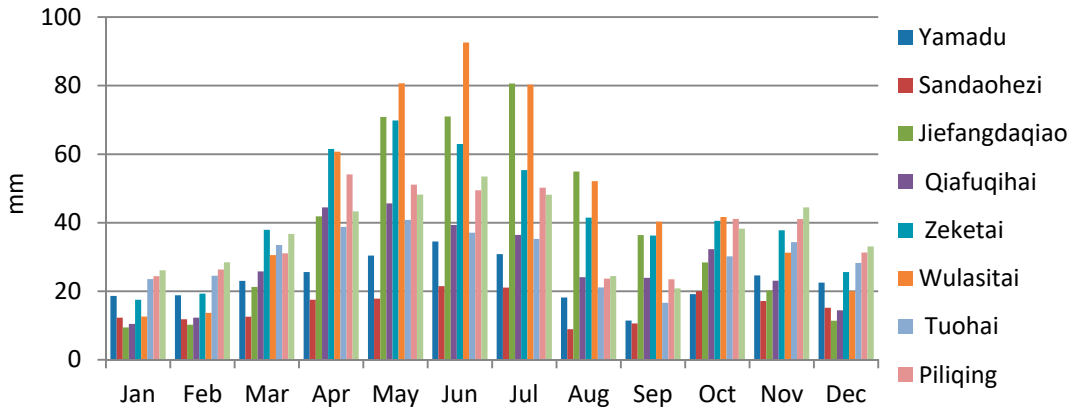


**Figure 2.** Annual cycle of precipitation in the research area for the selected meteorological stations. Locations of the stations is shown in Figure 1.

There are two different types of vertical distribution of annual precipitation in the study region [44]. In the more humid Kax and Kunes river basins, annual precipitation increases from 450–500 mm at the altitude 1000 m to 1200 mm at the climatic snow line elevation. Within the rest of the C-IRB territory, annual precipitation changes from 200–250 mm in the Ile Depression at an absolute elevation of 600 m a.s.l. to 780 mm at the altitude of the climatic snow line.

Summer precipitation accounts for about 60% of the annual precipitation, while precipitation falling from May to September accounts for over 80% of the annual total [39]. Both temperature and precipitation regimes can vary within the individual river basins due to complex orography. Figure 2 illustrates annual cycles of precipitation at different stations.

## 3. Data and Methods

### *3.1. Meteorological and Streamflow Data and Calculation of Trends*

Monthly data on temperature, precipitation, and streamflow were collected in the C-IRB at the stations listed in Table 1 and shown in Figure 1. These data were used for the analysis of the long-term trends and for the calculation of total glacier runoff and its components. Streamflow data from fours stations (Jiefangdaqiao, Qiedeke, Yamadu, and Zaketei) were used for trend analysis. Data from other stations were not used because of the insufficient length of the time series, large gaps in the data, or the modification of streamflow by dams and reservoirs.

**Table 1.** Hydrometeorological stations in the Chinese sector of the Ile River Basin (C-IRB). Locations of the stations are shown in Figure 1.

| Name | River | Altitude, m a.s.l. | Start Year | Missing Data | Area, km$^2$ | Glacierized Area, % |
|---|---|---|---|---|---|---|
| Yamadu | Ile | 700 | 1953 | 1954–1956 | 49,186 | 2.8 |
| Sandaohezi | Ile | 530 | 1989 | 1988–1990, 1992, 1994–2001 | 61,640 | 2.2 |
| Jiefangdaqiao | Tekes | 1640 | 1985 | 1985, 1986 | 8635 | 8.0 |
| Qiafuqihai | Tekes | 900 | 1956 | 1956 | 27,402 | 3.6 |
| Tehezhuan | Tekes | 1700 | 2002 | 2002–2004 | 6293 | |
| Zeketai | Kunes | 870 | 1960 | 1969–1971, 1974 | 4123 | 1.0 |
| Wulasitai | Kax | 1440 | 1957 | 2005–2010 | 5081 | 6.0 |
| Tuohai | Kax | 830 | 1953 | 1953–1954, 1993–1994 | 8656 | 3.6 |
| Piliqing | Piliqing | 860 | 1956 | 1994 | 794 | 0.0 |
| Qiedeke | Qiedeke | 940 | 1956 | 1968–1970 | 291 | 3.0 |
| Huiwuqiao | Khorgos | 1290 | 2003 | 2003 | 1160 | |

To examine long-term changes in precipitation and streamflow, the two-side Mann-Kendall (MK) test [45] was applied to monthly and seasonal data. The MK test is a non-parametric test with low sensitivity to abrupt breaks in the time series due to missing data [46].

Trend analysis was performed for two time periods, 1960–2010 and 1987–2010. The second period was used in order to include the Jiefangdaqiao station (Table 1).

### *3.2. Assessment of Changes in Glacier Area*

In order to assess temporal variability in glacier retreat rates, data from FCGI and SCGI for 1962–1963 [38] and 2007–2009 [39], respectively, were used, and new inventories for the Kuksu, Kunes, and Qiedeke basins were compiled for four time steps using Landsat imagery (Table 2).

**Table 2.** Satellite imagery used in this study. Source: United States Geological Survey Global Visualization Viewer [47].

| River Basin | Date | Satellite and Sensor | Resolution |
|---|---|---|---|
| Koksu | 2 August 1990 | Landsat 5TM | 30 m/15 m (multi-spectral/panchromatic) |
| | 22 August 1994 | | |
| | 31 August 2012 | Landsat 7 ETM+ | |
| | 7 September 2012 | | |
| | 1 August 2013 | Landsat 8 OLI TIRS | |
| Kunes | 2 August 1990 | Landsat 5TM | 30 m/15 m |
| | 28 August 1993 | | |
| | 22 August 1994 | | |
| | 31 August 2012 | Landsat 7 ETM+ | |
| | 7 September 2012 | | |
| | 29 August 2014 | Landsat 8 OLI TIRS | |
| Qiedeke | 20 September 1991 | Landsat 5TM | 30 m/15 m |
| | 13 August 2012 | Landsat 7 ETM+ | |
| | 11 August 2014 | Landsat 8 OLI TIRS | |

The FCGI and SCGI data were derived from the GLIMS database [48]. The mean uncertainty in the calculation of glacier area in FCGI and SCGI in the Ile basin was estimated as ±7.6% [40] and ±4.8% [39], respectively. The data of the glacier hypsometry for these two inventories were derived from the Randolph Glacier Inventory (RGI), versions 4.0 [49] for FCGI and 5.0 [50] for SCGI. In the new glacier inventories, glaciers in the same region as in FGGI were mapped and those mapped in FCGI were used for the calculation of glacier change.

All Landsat imagery was processed to level L1T by the distributor, i.e., it was orthorectified using a digital elevation model (DEM) and surface reference points. The dataset GLS2000 [51] served as the basis for geometric correction. The root-mean-square error ($RMSE_{x,y}$) in the GLS2000 data set was less than one pixel, which corresponds to an accuracy of ±30 m [51]. All images were re-projected into the 1984 WGS UTM projection, Zone 44. All images were acquired during the ablation period with minimum seasonal snow and cloud cover (Table 2). Most of the satellite images were of good quality, except several Landsat 7 images which had data gaps (showing as black stripes on the images). To overcome this problem, scenes from more than one acquisition in the same year were used, whereby the best quality scene was selected (Table 2).

ASTER GDEM2 [52] were used to derive river basin boundaries and to assist with determining morphological characteristics, boundaries, and aspects of glaciers. ASTER GDEM2 has horizontal resolution of 75 m and vertical resolution of 30 m. The overall vertical accuracy was determined by the ASTER GDEM validation team [52] as ±17 m at 95% confidence level. Previous assessments of ASTER accuracy in the Tien Shan using ground control points (GCP) confirmed that vertical accuracy of ASTER GDEM2 in the region is ±15 m [53].

Glacier outlines were mapped using the semi-automated band ratio methods (TM3/TM4 or OLI4/OLI5) with manual correction, by using the false-color composite bands TM 5, 4, 3 and OLI 6, 5, 4 [54–56]. Panchromatic images with spatial resolution of 15 m were used in manual corrections to decrease the mapping uncertainty. The uncertainty of glacier area change due to the co-registration of satellite images was determined using the buffer method described in [57]. The consecutive pairs of scenes were co-registered and a network of 10–15 tie points was established for each pair of scenes using clearly identifiable terrain features whose location did not change. The derived $RMSE_{x,y}$ values ranged between ±5.8 and ±6.2 m. A buffer with a width of half of $RMSE_{x,y}$ was created along the

glacier boundaries in the individual scenes, and the uncertainty term was calculated as an average ratio of the original glacier areas to the areas with a buffer increment. The accuracy of glacier mapping without manual correction ±4.3%, ±4.4%, and ±3.1% on the Landsat 8, 7, and 5 images, respectively. For those glaciers, whose outlines were corrected manually, the operator's error was calculated by the repeated delineation of 25 glaciers by several operators. For these glaciers, the mean uncertainty value was estimated as ±4.8% Landsat 8 and 7, and ±4.5% for Landsat 5.

In addition to glacier area, glacier length was measured as a distance between the top of the glacier and the terminus of its longest branch along the central flow line.

We note that in our hydrological analysis, glacier area data from the Chinese sector of the Tekes, Kax, and Khorgos river basins were used. This was obtained from the inventory published in [16], completed using the same methods and calculation of uncertainty as in this study.

### *3.3. Calculation of Runoff from Glacier Surface*

Runoff from glacier surface, including runoff formed due to the melt of seasonal snow, firn, and ice, was estimated using two methods: Degree-day model and empirical temperature-based index. In addition, runoff forming due to the melt of multiyear ice was calculated from changes in ice volumes between glacier inventories. These methods require information on the degree-day factors (DDFs) for snow and ice and knowledge of relative contribution of snow and ice melt in runoff from glacier surface which, in turn, require temperature and precipitation data as well as knowledge of regional vertical temperature gradients.

DDFs were calculated using Equation (1):

$$f = -a/\varphi, \quad (1)$$

where f is DDF, a is surface ablation (mm), and φ is a sum of positive temperatures (°C) over a selected period [58].

Mass balance measurements and high-elevation meteorological observations enabling the calculation of local temperature gradients are limited in the study area. We used the glaciological (stake) ablation measurements from the Tuyuksu Glacier (43°4′0″ N; 77°4′29″ E), which has been the World Glacier Monitoring Service (WGMS) reference glacier for Central Asia since 1957 ([17] and earlier years) to calculate the degree-day factors for snow and ice melt. At the Tuyuksu glacier, changes in surface elevation due to melt (accumulation) of snow and ice are measured using a network of 120 stakes at approximately 10-day intervals. These intervals were screened for the occurrence of liquid precipitation and those featuring liquid precipitation were excluded from analysis. Measurements from the 2008–2012 periods were used.

Vertical temperature gradients from the Ile Alatau were used to calculate changes in temperature with elevation and at the elevation of individual stakes. Temperature data were obtained from several meteorological stations located at different elevations leading to the Tuyuksu glacier [31], including the Tuyuksu meteorological station located at 3438 m a.s.l. A well-known step-change in temperature of −1 °C between the glacier ice and the surrounding terrain was accounted for when calculating the degree-day factors for ice but not for snow because of the assumption of a spatially continuous snow cover.

The mean values of snow and ice DDFs for the 2008–2012 period were −2.3 mm $°C^{-1}$ and −4.6 mm $°C^{-1}$, respectively. The worldwide average DDF value for snow was estimated as −4.1 ± 1.5 mm $day^{-1}$ $°C^{-1}$ [59] and values obtained in this study are low in comparison with DDFs reported for other glaciers located mainly in more humid regions of Europe, North America, and southern Asia [60]. DDF values vary considerably between and within regions, due to the relative importance of individual energy components providing energy for melt [60], and tend to be lower in dry regions (e.g., Central Asia) [60,61]. Negative nocturnal temperatures and summer snowfalls, typical of Tuyuksu, also tend to reduce DDF values.

3.3.1. Calculation of Runoff from Glacier Surface Using Degree-Day Model

The positive degree-day (PDD) method [60] was used for the calculation of runoff from the glacierized surface in the Qiedeke River basin for the 1961–2010 period, in line with the availability of the Qiedeke streamflow and runoff data (Table 1). Its steps are illustrated by Figure 3. The APHRODITE (Asian Precipitation—Highly Resolved Observational Data Integration Towards Evaluation of Water Resources) [62,63] reanalysis daily product version V1101 (for precipitation) and V1204R1 (for temperature) with spatial resolution of 0.25 degree were used for the study area. The spatial resolution of the APHRODITE reanalysis is too coarse to resolve spatial temperature variability with a glacier. Values of vertical temperature gradients from the Tuyuksu region (Section 3.3) were applied to estimate temperature change with elevation at a sub-grid scale.

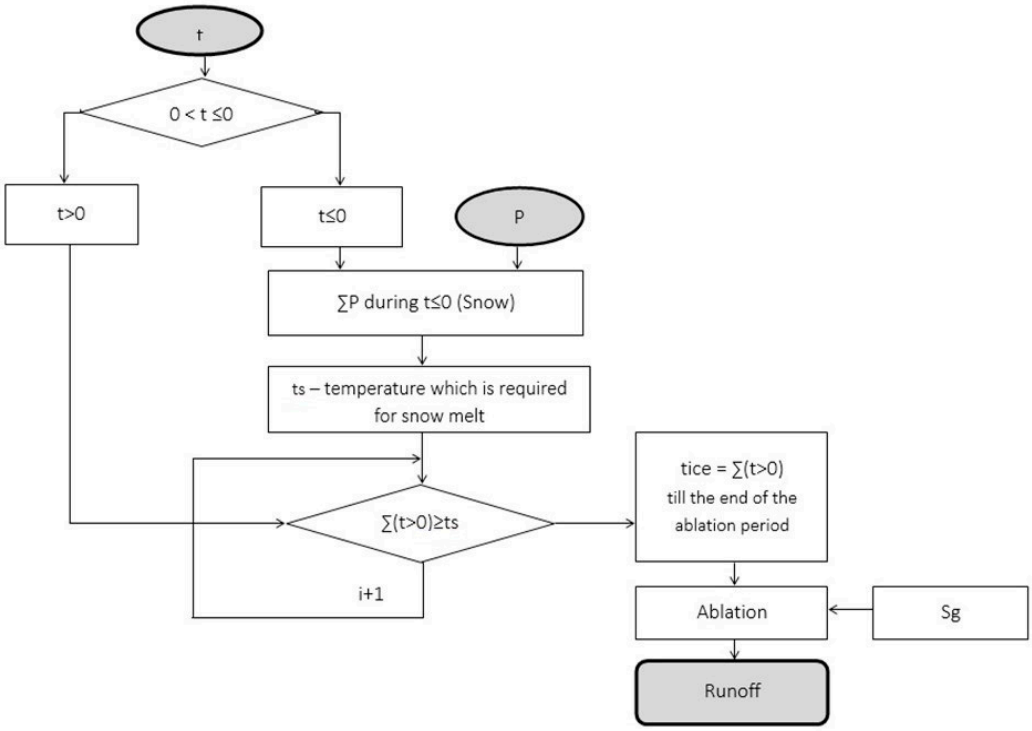


**Figure 3.** The scheme of the positive degree-day (PDD) glacier runoff model. t—daily temperature, P—daily precipitation, ts—sum of the temperature which is needed for complete snow melt, Sg—glacier area.

Using daily temperature data, the dates when temperature crossed a threshold of 0 °C were determined for autumn and spring. These dates were used to calculate a sum of solid precipitation over the cold period. Following the onset of positive temperatures in spring, sums of daily temperatures required for snow melt were calculated by using the DDF for snow (Section 3.3). Once this value had been reached, it was assumed that all snow had melted and the ablation of ice had begun. In the next step, a sum of positive daily temperatures was calculated up to the onset of negative temperatures in autumn. Ice ablation during the warm period was calculated as a product of the sum of positive temperatures during the assumed period of ice melt and the DDF for ice (Section 3.3). This method enables separate calculation of snow melt and ice melt.

#### 3.3.2. Calculation of Glacier Runoff Using Temperature-Index Method

Glacier runoff using the empirical Krenke-Khodakov temperature-index Equation (2) based on the assumption that annual accumulation at the ELA is equal to the ablation which constitutes runoff from glacierized surface including snow and ice melt [64]:

$$A = 1.33(t_s + 9.66)^{2.85} \quad (2)$$

where A is annual accumulation at ELA (mm water equivalent (w.e)); and $t_s$ is average summer (June to August) air temperature (°C), calculated using air temperature obtained from the nearest weather stations, environmental lapse rate a step change in temperature of 1 °C between glacier and ice-free surface. The uncertainty of the calculation of l runoff using this method is estimated as 16 g/cm$^2$ (11%) [64].

#### 3.3.3. Calculation of Glacier Runoff from Changes in Ice Volume

The amount of runoff formed due to the melt of multiyear ice was estimated as the loss of ice volume (expressed as water equivalent using ice density of 900 kg m$^{-3}$) between the consecutive glacier inventories. A range of empirical power-law scaling equations are available and used as a simple and robust method for estimating glacier volume from observations of area [65–69] and many others. In this study, we used the same scaling relationships as in FCGI to maintain consistency with this study for three periods of glacier area assessment [8,38]:

$$H = 53.21 \times S^{0.3} - 11.23 \quad (3)$$

$$H = 34.4 \times S^{0.45} \quad (4)$$

where H is the glacier thickness (m) and S is the glacier area (km$^2$). Equation (3) is used for cirque, valley-cirque, and valley glaciers, and Equation (4) is used for hanging glaciers. Following the estimation of glacier thickness, ice volume was calculated as:

$$V_g = S \times H/1000 \quad (5)$$

where $V_g$ is the glacier ice volume (km$^3$).

#### 3.3.4. Separation of Runoff Components

The term 'glacier runoff' has varying meanings in literature on glacier hydrology of Central Asia [1,2,70,71]; (Section 1). A more precise definition is 'runoff from glacier surface' which is comprised by runoff formed by the melt of snow, firn, and ice (in the ablation zone and under the moraines), and subglacial drainage and liquid precipitation flowing into the river network from glacier surface [72]. The relative contributions of these components are poorly quantified in Central Asia [2]. Examples of existing studies include empirical hydrograph separation by [73], and attempts of separation based on isotopic analysis—which, so far, have been based on limited sampling [74–77]. Sosedov [70] modeled mean values of the components of glacier runoff in the northern Ile Alatau using data from the glacier inventory of 1955 and mass balance data from the Tuyuksu glacier for 1957–1974. The estimated relative contributions of different components [70] are shown in Table 3. It was shown that approximately 60% of glacier runoff is contributed by the melt of solid precipitation accumulated during the current balance year (components s and f in Table 3). The share of subglacial melt water is two–three orders of magnitude lower than any other component of glacial runoff, and is usually not considered in the assessment of water balance.

**Table 3.** Average value of glacier runoff components at the northern slope of the Ile Alatau [70].

| Glacier Runoff Components | Index | Runoff Volume | |
|---|---|---|---|
| | | $10^9$ m$^3$ | % |
| Snow melting at the firn area | f | 41.8 | 16.1 |
| Snow melting at the terminus | s | 114.5 | 44 |
| Ice melting at the terminus | g | 101.9 | 39.1 |
| Ice melting under the moraine | j | 2.2 | 0.8 |
| Total | | 260.4 | 100 |

When mass balance of a glacier is close to zero or positive, glacial runoff is entirely determined by the precipitation of the current year. In this case, it is justified to equate annual accumulation at the ELA to ablation across the glacier area and to glacial runoff [78,79]. However, during the period of intensive glacier wastage, observed in Central Asia since the 1970s, this balance is violated and melting of multiyear ice becomes an important component of glacial runoff. Thus, during the period of 1961–2012, mean glacier mass change in the C-IRB was −0.5~−1.0 $10^3$ kg m$^{-2}$ a$^{-1}$ [13].

Our monitoring of snow and ice melt on the Tuyuksu glacier (Section 3.3) showed that relative contributions of runoff components, shown in Table 3, have changed during the period of intensive degradation of glaciers. On average, between 1998 and 2016, the snow (f and s in Table 3) component accounted for 33% (475 mm) of runoff from the glacier surface, while the ice component (g and j) accounted for 67% (1213 mm). This proportion was used in this study to calculate relative contributions of snow and ice in runoff from glacierized surface. We note that during the years with strong positive temperature and negative precipitation anomalies (e.g., 2008, 2014), ice melt accounted for as much as 90% of the total glacier runoff. Similar temperatures were observed in the region in the 1970 [31], suggesting a similarly high contribution from ice melt.

It was assumed that all liquid precipitation runs off glacier surface. Liquid precipitation is a relatively small component of runoff from glaciers in Central Asia and accounts for no more than 7% of its total value [64]. Evaporation losses from the snow-ice surface in the study area are balanced by condensation [19,80].

## 4. Results

### *4.1. Changes in Glacier Area in the Kuksu, Kunes, and Qiedeke River Basins*

The statistics of, and changes in, glacier area observed in the Kuksu and Kunes river basins at different time steps are shown in Tables 4 and 5. The FCGI data for the Qiekeke River basin included only 19 glaciers with a total area of 14.02 km$^2$, which declined by 2% in 1991 (0.1% a$^{-1}$) and by 31% in 2014 (0.6% a$^{-1}$) in comparison with the 1962/63 survey.

**Table 4.** Changes in glacier number, total area, and minimum elevation of glacier tongues averaged over the samples.

| Year | Number | Area, km$^2$ | H min, m | Number | Area, km$^2$ | H min, m |
|---|---|---|---|---|---|---|
| | Kuksu | | | Kunes | | |
| 1962/63 | 625 | 421.6 | 3680 | 250 | 96.7 | 3554 |
| 1990 | 648 | 376.8 ± 11.3 | - | - | - | - |
| 1993 | - | | - | 240 | 81.5 ± 2.4 | - |
| 2007/09 | 493 | 293.5 ± 14.1 | 3761 | 193 | 51.8 ± 2.5 | 3615 |
| 2011/12 | 638 | 279.2 ± 8.4 | 3746 | 193 | 52.4 ± 1.6 | 3615 |

**Table 5.** Area and changes in the extent of clear ice in the Kuksu and Kunes river basins.

| **Year** | **1960s** | **1990s** | **2010s** |
|---|---|---|---|
| Area, km$^2$ | 518, 3 | 450, 4 | 326, 9 |
| **Period** | **1960s–1990s** | **1990s–2010s** | **1960s–2010s** |
| Area change, km$^2$ | 67.8 ± 5.9 | 123.5 ± 10.9 | 191.3 ± 16.8 |
| Rate, km$^2$ a$^{-1}$ | 2.4 ± 0.2 | 5.6 ± 0.5 | 3.9 ± 0.3 |
| Area change, % | 13.1 ± 8.8 | 27.4 ± 8.4 | 36.9 ± 6.5 |
| Rate, % a$^{-1}$ | 0.5 ± 0.003 | 1.2 ± 0.003 | 0.8 ± 0.001 |

In the much more heavily glacierized Kuksu and Kunes basins, between 1962/63 and 2011/12, glaciers lost 186.7 km$^2$ or 36% (0.8% a$^{-1}$) overall. We found 56 small glaciers, which were not registered by FCGI, with a total area of 4.7 km$^2$. These glaciers were excluded from analysis for consistency with the FCGI data. Between 1962 and 2012, 245 glaciers with a combined area of 38.97 km$^2$ (or 7.5% of the total glacierized area as in 1962/63) melted completely. Of these, 141 glaciers with a total area of 19.4 km$^2$ disappeared between 1962/63 and 1993, and 104 between 1993 and 2012. In the 1962/63–1990/93 and 1990/93–2012 periods, 53 and 110 glaciers, respectively, split (86 and 24 glaciers in Kuksu and Kunes river basins). Between the 1960s and the 2010s, glacier length has declined on average by 300 m, from 1.14 km to 0.84 km.

Changes in the extent of glacier areas are shown in Tables 4 and 5. The total glacier area in both river basins decreased by 191.30 km$^2$ (36.9%) between the FCGI and SCGI. However, within this period, glacier retreat intensified substantially. Between 1990/92 and 2012, glaciers in both basins on average lost area at a rate of 1.4% a$^{-1}$, while between 1962/63 and 1990/92, the rate of area reduction was 0.5% a$^{-1}$.

In both river basins, over 70% of all glaciers have areas less than 0.5 km$^2$. In 2012, in the Kunes basin, these glaciers accounted for approximately 40% of the total glacierized area. In the Kuksu basin, glaciers with individual areas of 2.0–5.0 km$^2$ prevailed and had the highest share (23%) of the total glacierized area. The mean glacier area declined from 0.68 km$^2$ to 0.44 km$^2$ and from 0.39 km$^2$ and 0.27 km$^2$ in the Kuksu and Kunes basins, respectively, between 1962/63 and 2012/13.

In the 2010s, in both basins, hanging glaciers dominated by number (48%); however, the largest area (158.7 km$^2$ or 48%) was occupied by valley and cirque-valley glaciers (Figure 4a). Most glaciers (76%) have northern aspect and cover more than 80% of the total glacier area (Figure 4b). Distribution of glaciers by elevation at the three steps of assessment is shown in Figure 4c.

Similar to the other regions of the Tien Shan [2,5,11,25,26,81–83], the rates of glacier area loss depended on the initial size of glaciers (Table 6; Figure 5). The largest absolute loss characterized larger glaciers. Small glaciers (≤1 km$^2$), located at all elevations, exhibited the largest relative area reduction. Between the 1960s and 2010s, the small glaciers lost over 40% of their total area. The medium-size glaciers (2–10 km$^2$) lost 26–31% of their area. There were only two glaciers with individual areas in excess of 10 km$^2$, and it is difficult to evaluate area change in this class.

While degradation of glaciers in all size classes less than 10 km$^2$ intensified between the 1990s and the 2000s, the strongest increase in glacier area loss rate characterized the smallest glaciers with individual areas under 0.5 km$^2$ (Table 6; Figure 5). We note that in the 1960s–90s, the rate of relative change in area of these very small glaciers was lower than that of glaciers with an area between 0.5 km$^2$ and 1 km$^2$. A possible explanation of this discrepancy is uncertainty of the FCGI assessment, which was higher for very small glaciers [40]. The range of individual glacier area reduction of all glaciers varied widely between 4% to complete melt, depending on the specific features of local topography.

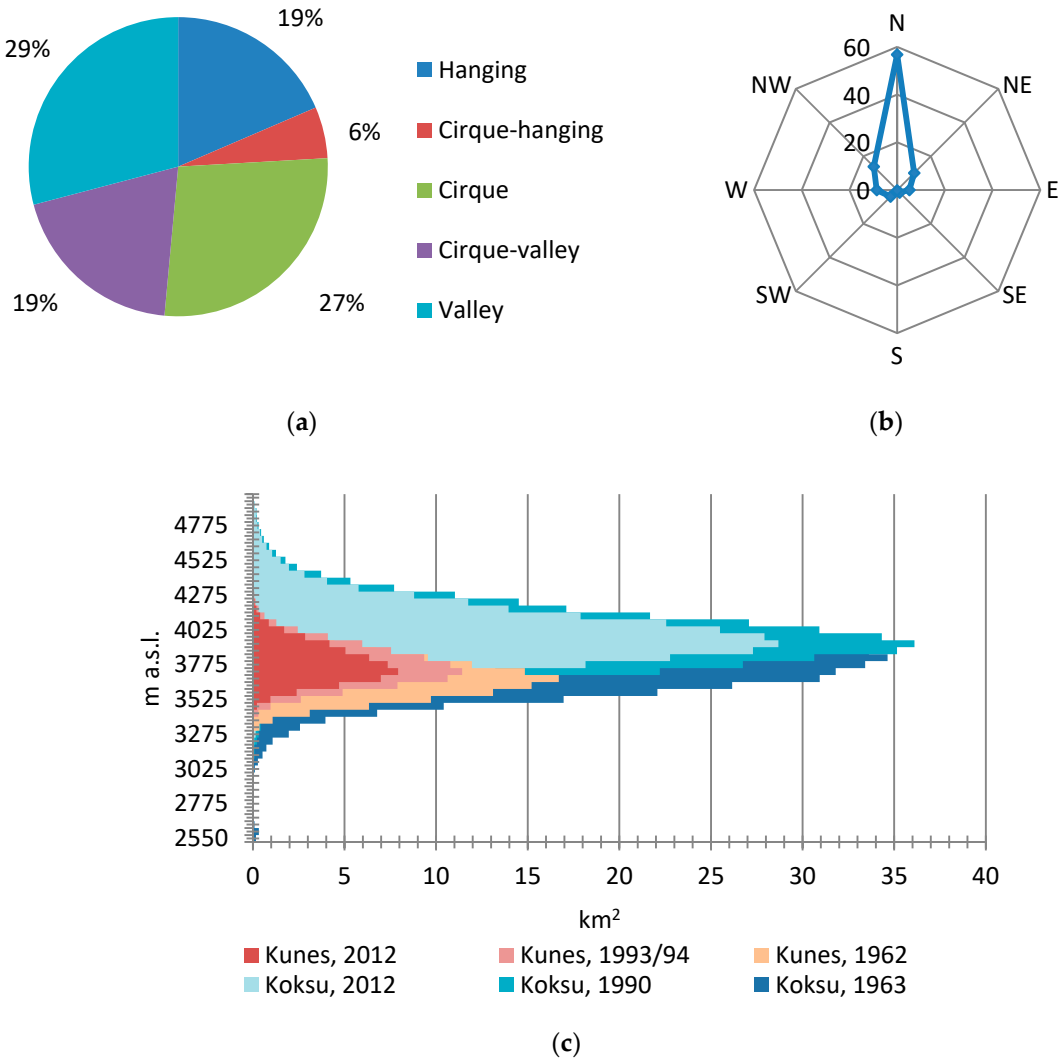


**Figure 4.** Distribution of glacier area by type (**a**), aspect (**b**) in 2010s, and elevation in 1960s, 1990s, and 2010s (**c**).

**Table 6.** Changes in glacier area by size class.

| Size Class, km² | Number 1962/63 | Total Clear Ice Area, km² | | | | Area Loss, %/(% a⁻¹) | | |
|---|---|---|---|---|---|---|---|---|
| | | 1962/63 | 1990/93 | 2007/09 | 2012/13 | 1960s–1990s | 1990s–2010s | 1960s–2010s |
| ≤0.5 | 634 | 116.8 ± 8.9 | 105.1 ± 4.7 | 52.7 ± 2.5 | 62.7 ± 3.0 | 10 (0.4) | 40 (3.3) | 46 (0.9) |
| 0.51–1.0 | 118 | 83.1 ± 6.3 | 63.4 ± 2.9 | 46.3 ± 2.2 | 43.5 ± 2.1 | 24 (0.9) | 31 (2.6) | 48 (1.0) |
| 1.01–2.0 | 65 | 87.9 ± 6.7 | 71.1 ± 3.2 | 54.1 ± 2.6 | 50.6 ± 2.4 | 19 (0.7) | 29 (2.4) | 42 (0.9) |
| 2.01–5.0 | 46 | 136.7 ± 10.4 | 128.7 ± 5.8 | 111.1 ± 5.3 | 101.5 ± 4.9 | 6 (0.2) | 21 (1.8) | 26 (0.5) |
| 5.01–10.0 | 10 | 65.3 ± 5.0 | 56.4 ± 2.5 | 51.9 ± 2.5 | 44.9 ± 2.2 | 14 (0.5) | 20 (1.7) | 31 (0.6) |
| 10.01–15.0 | 1 | 10.2 ± 0.8 | 10.6 ± 0.5 | 9.8 ± 0.5 | 9.9 ± 0.5 | +4 (+0.1) | 7 (0.6) | 3 (0.1) |
| >15 | 1 | 18.2 ± 1.4 | 15.2 ± 0.7 | 17.1 ± 0.8 | 13.9 ± 0.7 | 17 (0.6) | 8 (0.7) | 23 (0.5) |
| Total | 875 | 518.3 | 450.4 | 343.1 | 326.9 | 13.1 (0.5) | 27.4 (1.2) | 36.9 (0.8) |

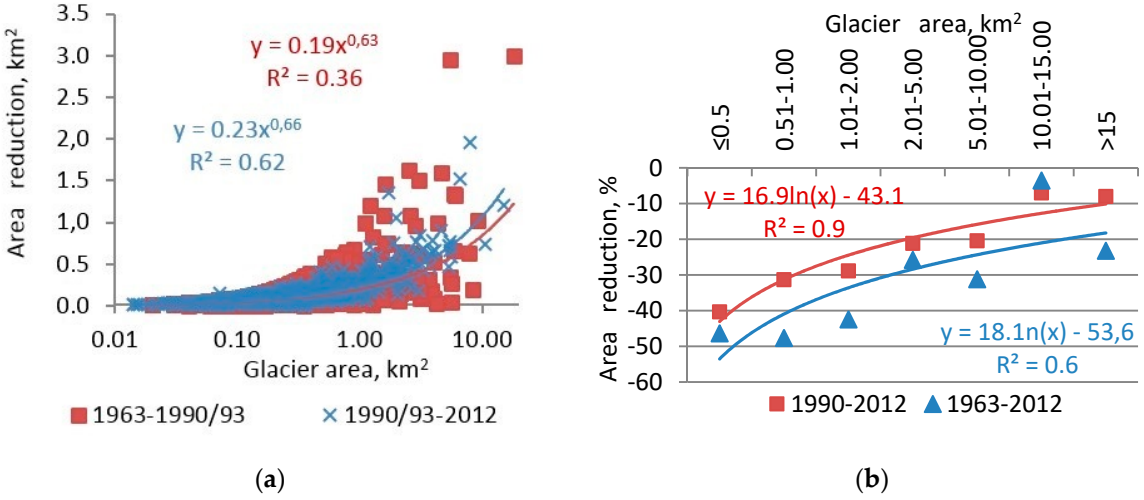


(**a**) (**b**)

**Figure 5.** Scatter plot of (**a**) absolute glacier area loss and (**b**) relative area loss over the two assessment periods versus the initial glacier areas as in 1962/63 and 1990/93.

Changes in areas of glaciers of different types are in agreement with changes in area of glaciers of different size. The biggest relative loss (48–54%) of area characterized the cirque-hanging and hanging glaciers, which are usually small (Figure 5a) and are considered to be more sensitive to climate change than other types of glaciers [15,84]. In absolute terms, the largest wastage rate characterized larger valley glaciers, which is typical of the Tien Shan [10,25]. The cirque-valley and valley glaciers lost 26–29% of their initial areas, which is less than glaciers of other types (Figure 6a). There is a notable difference between temporal trends in the wastage of glaciers of different types. Area loss of cirque, cirque-valley, and valley glaciers intensified from the 1990s, with the latter two experiencing twice as much relative area loss in the 1990s–2010s than in the 1960s–1990s. By contrast, and despite a larger overall relative reduction in area, there was no change in the rate of relative area loss of the cirque-hanging and hanging glaciers, possibly due to the protective influence of the topographic features favorable for their existence and/or uncertainties of FCGI.

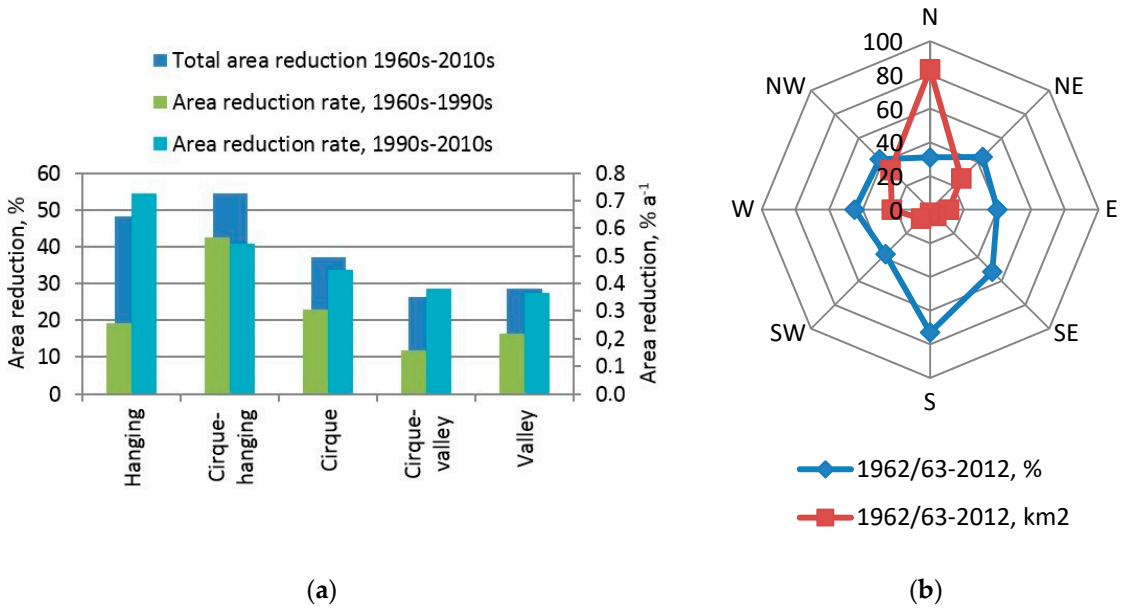


(**a**) (**b**)

**Figure 6.** Glacier area loss (**a**) by morphological types as percentage of the initial glacier area and per year for the two assessment periods, and (**b**) by aspect.

Over the entire period, in relative terms, the highest area loss characterized glaciers located on slopes with southern (73%) and south-eastern (52%) aspect, while the lowest area loss (31%) characterized glaciers with northern aspect (Figure 6b). In absolute terms, glaciers located on the north-facing slopes lost more because they dominate in the region (Figure 6b).

Between the 1960s and 2010s, the mean elevation of glacier tongues increased by 49 ± 15 m and 60 ± 15 m in the Koksu and Kunes river basins, reaching 3745 m a.s.l. and 3615 m a.s.l., respectively (Figure 4c).

Figure 7 illustrates the relationship between changes in glacier areas and elevation of glacier tongues. The largest reduction characterized glaciers with the lowest elevation, especially those whose tongues were positioned below the mean regional ELA. At the same time, the existence of small glaciers at all elevations (as well as the response of hanging or cirque-hanging glaciers discussed above) shows their capacity to adjust to the changing of climate conditions in the favorable topographic setting. We also note that glaciers located in the intermountain basins showed lower sensitivity to the observed climate change. This is probably due to the difference in the ELA: In the outer ranges of the Tien Shan, the ELA is positioned at 3550–3600 m, while in the intermountain regions, it reaches 4500 m [1,78].

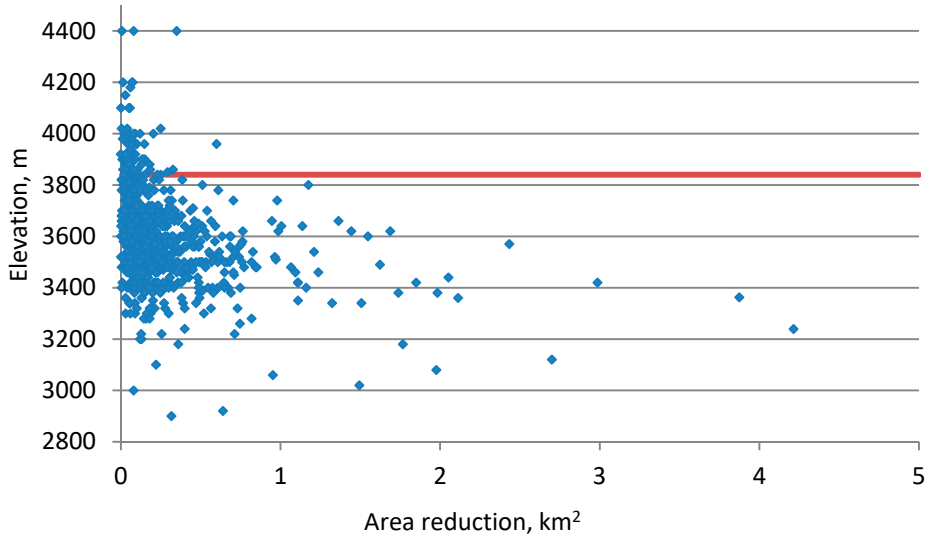


**Figure 7.** Absolute changes in glacier area versus the elevation of glacier termini between 1962/63 and 2012. Red line is mean regional ELA.

### *4.2. Changes in Streamflow*

Figure 8 illustrates annual cycles of streamflow of five of the studied rivers. The river nourishment varies depending on the characteristics of the catchments and location of the gauging sites. Thus, precipitation and ground-water nourishment predominate in the non-glacierized Piliqing catchment where streamflow peaks in spring, following snow melt. Similarly, at the Zeketai station, the Kunes River is nourished predominantly by precipitation and its flow peaks in spring, following snow melt and in line with precipitation maximum. Streamflow of these two rivers exhibits a strong correlation with precipitation (Table 7). The Tekes catchment, represented here by the Jiefangdaqiao station, has the highest glacierization (Table 1) and its streamflow peaks in July and August, when glaciers melt. Its streamflow, as well as that of the Ile at the Yamadu station and Qiedeke which also peak in summer, exhibit moderate correlation with precipitation but strong correlation with air temperature (Table 7).

The time series of seasonal streamflow and results of the MK test are shown in Figures 9 and 10, respectively. There were no statistically significant (at 95% confidence level) linear trends in streamflow in most months at three out of four gauging sites. At the Yamadu site, positive trends were registered in autumn (SON: $\tau = 0.21$, $p = 0.04$), winter (DJF: $\tau = 0.30$, $p = 0.01$), and early spring (MAM: $\tau = 0.20$, $p = 0.04$) during the 1960–2010 and 1987–2010 periods. During the latter period, the increase was

stronger than over the whole period of observations. A strong increase in the spring streamflow was evident from the mid-1990s, possibly indicating stronger and earlier snow melt and its contribution to discharge. Positive trends in winter streamflow were registered at Jiefangdaqiao (DJF: $\tau = 0.116$, $p = 0.050$) from 1987 (similarly to the catchments with high glacierization in the northern Tien Shan [31] and at the Zeketai station during the 1960–2010 period). At Zeketai, however, trends in winter streamflow were inconsistent between the shorter and the extended periods of assessment.

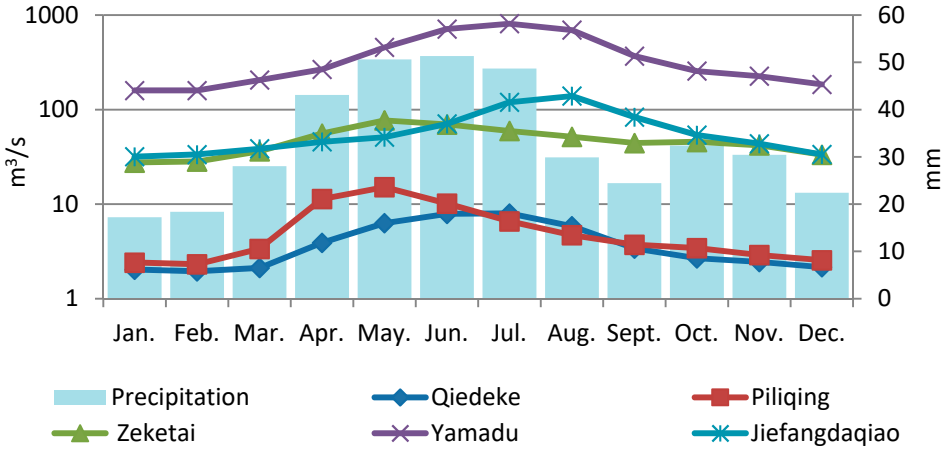


**Figure 8.** Precipitation (mm) and streamflow ($m^3$ $s^{-1}$) averaged over the 1960–2010 period for different stations. Locations of the stations are shown in Figure 1.

**Table 7.** Mean annual streamflow, mean of annual sum of precipitation and Pearson correlation coefficient between monthly streamflow and monthly precipitation and temperature for the 1960–2010 period.

| Station | Streamflow, $m^3$ $s^{-1}$ | Precipitation, mm | Correlation of Streamflow and Precipitation | Correlation of Streamflow and Temperature |
|---|---|---|---|---|
| Qiedeke | 4.1 | 445 | 0.57 | 0.87 |
| Piliqing | 5.7 | 447 | 0.77 | 0.57 |
| Zeketai | 47.6 | 506 | 0.96 | 0.84 |
| Yamadu | 374.8 | 278 | 0.49 | 0.87 |
| Jiefangdaqiao | 62.0 | 457 | 0.68 | 0.77 |

During the warm period, statistically significant negative trends were registered in June at the Jiefangdaqiao station during 1987–2010, and in August at the Qiedeke station over the entire assessment period (Table 1). Streamflow in June is dominated by snow melt, while in August, the ice melt component dominates. It appears that the small Qiedeke catchment is affected despite the low glacierization of 3% (Table 1).

The observed long-term changes and shorter-term variability in streamflow are consistent with those observed in other regions of the Tien Shan [31]. Thus, in northern Tien Shan, positive trends were registered in autumn and winter across the region, and in spring at lower elevations, while there were no significant trends in summer streamflow except positive trends in the catchments with high (over 10%) glacierization. In all study catchments, a decrease in streamflow was observed in the mid-1970s–1980s. This is also consistent with variability in streamflow in northern Tien Shan and Jungar Alatau, which was attributed to changes in atmospheric circulation and associated negative anomalies in precipitation [31].

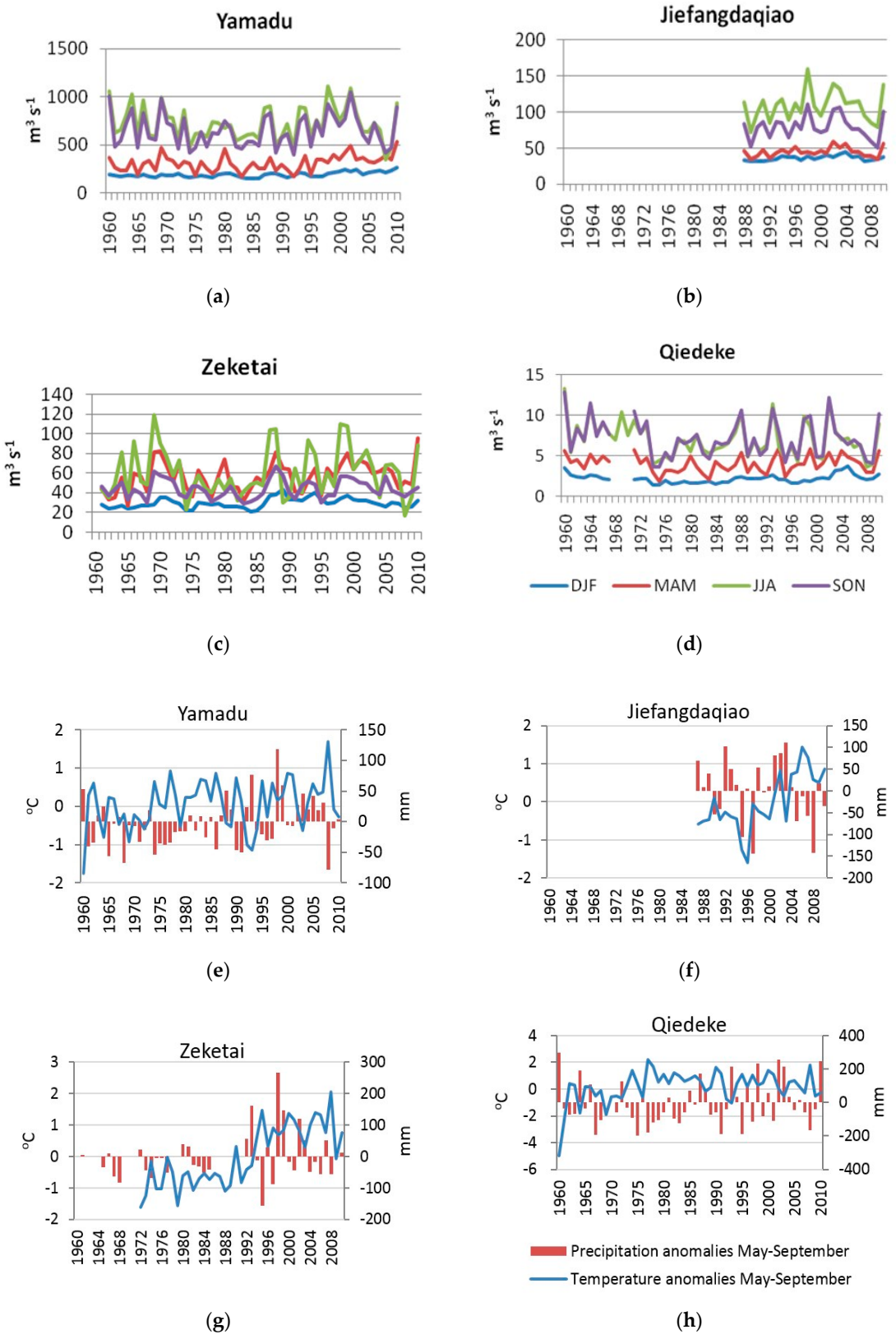


**Figure 9.** Time series of seasonal mean streamflow ($m^3$ $s-^1$) (**a**–**d**) and precipitation and temperature anomalies during the warm season (May to September) (**e**–**h**). Note that different scales are used for different rivers.

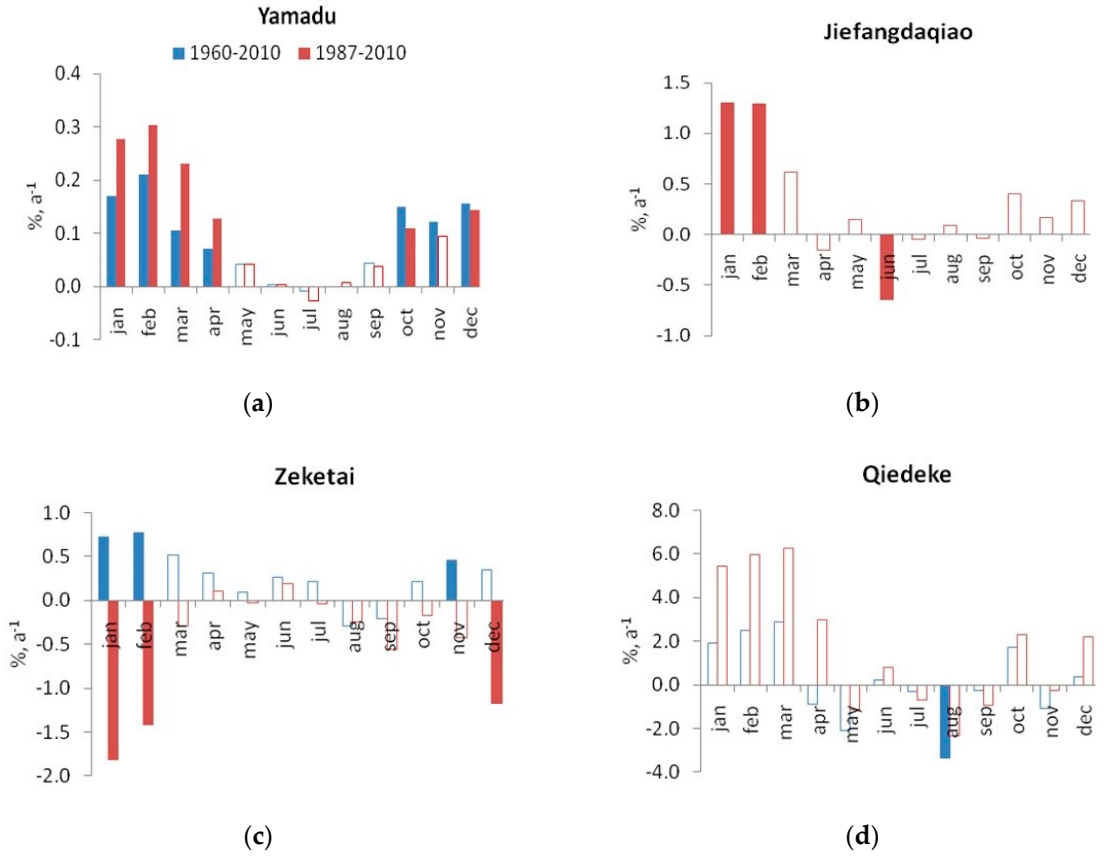


**Figure 10.** Trends in monthly streamflow (% $a^{-1}$) over the two periods of individual records calculated using the Mann-Kendal test for Yamadu (**a**), Jiefangdaqiao (**b**), Zeketai (**c**) and Qiedeke (**d**) stations. Solid bars represent trends significant at 0.05 confidence level. Different scales are used for different rivers.

### *4.3. Runoff from Glacier Surfaces Calculated by PDD and Temperature-Index Methods*

The glacier runoff in the Qiedeke catchment was analyzed by two methods, PDD and temperature index (Sections 3.3.1 and 3.3.2). The results from the application of the PDD method are presented for ice melt, while the results of the temperature-index methods show combined snow and ice runoff. The PDD method shows that mean runoff generated by melting of glacier ice during 1962–2010 was $26.3 \times 10^6$ $m^3$ $a^{-1}$ (Figure 11). The Krenke-Khodakov method showed that mean total runoff from the glacier surface (including snow and ice melt) during the same period was $17.0 \times 10^6$ $m^3$ $a^{-1}$ (Figure 11). A discrepancy in absolute values of runoff, calculated using these two methods, is significant, with the PDD method generating higher runoff values despite the fact that this is runoff generated by ice melt only. However, both runoff time series exhibit very similar temporal trends, possibly because both are driven by the same temperature data set. The MK test showed that there was a significant negative trend in both time series between 1962 and 2010, with a $\tau$ value of −0.27 and coefficients of determination of 0.20–0.22.

The temperature-index method was only applied to the Zeketai and Yamadu data sets, with calculation for the Zeketai station being limited to the period of 1972–2010 due to the availability of temperature data (Table 1, Figure 9). The MK test showed significant positive trend ($\tau = 0.27$, $p = 0.02$) in the total glacier runoff at the Zeketai station for the 1972–2010 period, and significant negative trend ($\tau = -0.18$, $p = 0.01$) for the Yamadu station during 1960–2010. The significant positive trend in the total glacier runoff could be explained by the significant positive trend of temperature ($\tau = 0.56$, $p = 0.001$) at this station, which is positioned at a higher elevation than the Yamadu station ($\tau = -0.13$, $p = 0.24$). The mean share of runoff from the glacierized surfaces during the warm period (May to September) was

24% for Qiedeke, 17% for the Ile at Yamadu, and 8% for the Kunes at Zeketai (Figure 10). The Quideke catchment is the smallest of all, and despite a relatively low glacierization of 3% (Table 1), runoff from glaciers appears to be a dominant source of nourishment. Importantly, it was runoff from glaciers that sustained the river flow in the 1970s when strong positive anomalies in temperature and negative anomalies in precipitation were observed across the Tien Shan [31], and particularly in 1974 and 1977 when positive June-July-August (JJA) temperature anomalies of 1.4 °C and 2.2 °C were registered at the Qiedeke station.

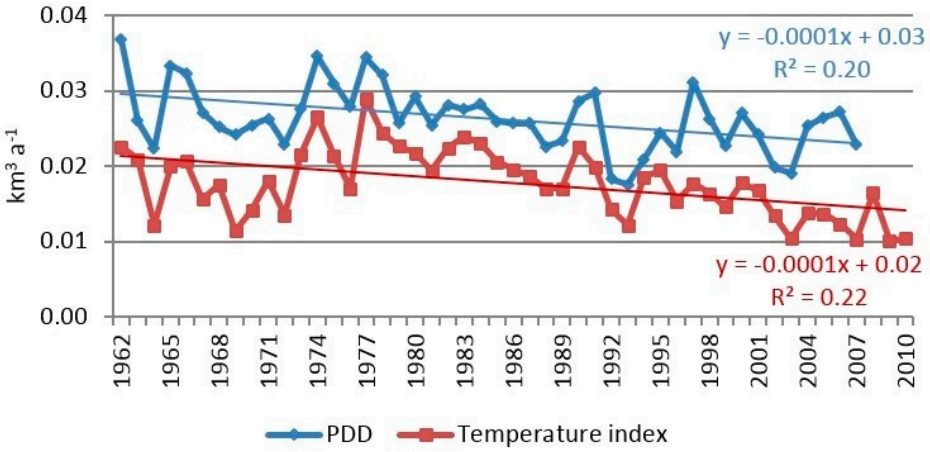


**Figure 11.** Glacier runoff by the PDD and the temperature-index methods Qiedeke.

### *4.4. Calculation of Runoff from Melting of Muli-Year Ice from Changes in Ice Volume*

Runoff generated by melting of the multiyear ice and its contribution to river runoff was calculated from changes in glacier volume (Section 3.3.3) for the Yamadu station, because this gauging site is located further downstream on the Ile river. In order to calculate changes in glacier volume affecting runoff measured at Yamadu, changes in glacier area and volume for the Khorgos, Kax, and the Chinese sector of the Tekes basin were required, in addition to the Kuksu and Kunes basins. These were obtained from previous assessments [16] and are shown in Tables 8 and 9. In all, 58.4 km$^3$ of glacier ice was lost between 1962 and 2012 in this sector of the Ile basin (Table 9). The relative loss of volume varied between 31% in the Kax sub-basin and 51% in the Khorgos sub-basin. This lost ice volume, converted into water equivalent, constitutes a component of runoff formed through the loss of multiyear ice (Table 10). As shown in Section 3.3.4, under the condition of rapid glacier retreat, this component represents 67% of the total runoff from the glacierized surface, while snow and firn melt contributes 33%. The total runoff from the glacierized surface was estimated using this ratio (Table 10).

**Table 8.** Glacier ice area (km$^2$) in C-IRB.

| Basin | 1962/63 | 1990 | 2000 | 2007 | 2008 | 2011 | 2012 |
|---|---|---|---|---|---|---|---|
| Khorgos | 55.2 | 45.3 | 41.7 | 30.7 | 32.2 | 31.6 | 31.4 |
| Kax | 421.6 | 359.2 | 336.9 | 314.1 | 316.8 | 311.5 | 309.7 |
| Kunes | 96.7 | 82.9 | 69.0 | 51. 8 | 57.5 | 56.6 | 52.4 |
| Kuksu | 421.6 | 376.8 | 342.0 | 293.5 | 314.3 | 309.1 | 279.2 |
| Tekes | 1027.6 | 852.4 | 789.9 | 847.8 | 709.3 | 697.4 | 693.5 |

**Table 9.** Changes in the extent of glacier ice and volume in the main sub-basins of C-IRB between 1963 and 2011/12.

| Basin | Area Loss | | Ice Volume, km$^3$ | | Ice Volume Loss | |
|---|---|---|---|---|---|---|
| | km$^2$ | % | 1963 | 2011 г. | km$^3$ | % |
| Kax | −104.8 | −25 | 28.17 | 19.55 | −8.62 | −31 |
| Kunes | −40.1 | −41 | 3.45 | 1.76 | −1.68 | −49 |
| Kuksu | −112.5 | −27 | 23.08 | 14.15 | −8.94 | −39 |
| Tekes | −330.2 | −32 | 85.35 | 46.19 | −39.15 | −46 |
| Total | −611.0 | −30 | 142.18 | 82.69 | −59.49 | −42 |

**Table 10.** Change in the share of total glacier runoff in the Ile river runoff at the Yamadu station. $Q_{gl}$—runoff from melting of multiyear ice; $Q_{gr}$—total glacier runoff; Veg. period—vegetative period between May and September.

| Time Period | Measured River Runoff | | | | $Q_{ice}$ km$^3$ a$^{-1}$ | % of $Q_{ice}$ in $Q_{river}$ | | Liquid Precipitation km$^3$ a$^{-1}$ | $Q_{glacial}$ km$^3$ a$^{-1}$ | % of $Q_{glacial}$ in $Q_{river}$ | |
|---|---|---|---|---|---|---|---|---|---|---|---|
| | Year | | Veg. Period | | | Year | Veg. Period | | | Year | Veg. Period |
| | $Q_{river}$ m$^3$ s$^{-1}$ | V km$^3$ | $Q_{river}$ m$^3$ s$^{-1}$ | V km$^3$ | | | | | | | |
| 1963–1991 | 347.9 | 11.0 | 511.4 | 8.1 | 1.5 | 13.6 | 18.5 | 0.18 | 2.4 | 21.8 | 29.6 |
| 1992–2000 | 391.1 | 12.4 | 579.3 | 9.2 | 1.4 | 11.3 | 15.2 | 0.15 | 2.3 | 18.1 | 24.3 |
| 2001–2007 | 422.6 | 13.4 | 608.6 | 9.6 | 2.2 | 16.4 | 22.9 | 0.22 | 3.5 | 26.2 | 36.5 |
| 2008–2011 | 399.1 | 12.6 | 531.1 | 8.4 | 0.6 | 4.8 | 7.1 | 0.06 | 0.95 | 7.5 | 11.3 |
| Mean | 391.5 | 12.4 | 567.4 | 8.9 | 1.4 | 11.6 | 15.9 | 0.16 | 2.31 | 18.5 | 25.3 |

The highest per annum contribution of the melting multiyear ice to the Ile runoff of 2.2 km$^3$ a$^{-1}$ was observed during the 2001–2007 period (Table 10), during the period of high positive temperature anomalies at all of the stations (Figure 9e–h). The highest relative contributions characterized the 1963–1994 and 2001–2007 periods, when this component accounted for 18.5% and 22.9% of the Ile flow, respectively. The high contribution of the multiyear ice melt in the former period is due to a relatively low flow of the Ile (Figure 7), due to the drought conditions, while contribution of the multiyear ice melt was close to average. The high contribution in the latter period is due to a sharp increase in glacier shrinkage in the region as a whole [16], reaching 1.2% a$^{-1}$ in the Kuksu and Kunes basins (Table 4). More recently, in the 2008–2011 period, runoff due to the melt of multiyear ice declined to 0.6 km$^3$ a$^{-1}$. This period, however, is very short and re-evaluation may be required for extended years. Overall, in 2001–2011, runoff formed due to the melt of the multiyear ice showed the same values as in the 1990s, but its values declined in the 1980s in comparison with the earlier years. This change in means is statistically significant at the 0.05 confidence level.

## 5. Discussion

This study assessed changes in the extent of clear glacier ice in the Kuksu, Kunes, and Qiedeke basins at several time steps. The results contribute to the knowledge of glacier change in the Tien Shan in two ways. Firstly, they enable an assessment of changes in the rates of glacier retreat between FCGI and SCGI [38,39]. Secondly, they complete the assessment of glacier change in the C-IRB, enabling assessment of impacts of climate and glacier change on the Ile runoff and water availability in this arid region.

The mean rate of glacier area loss in the Kuksu and Kunes basisns was 0.8% a$^{-1}$ between FCGI and SCGI when the region lost 36.9 ± 6.5% of glacier area overall. Within this period, however, glacier shrinkage intensified from 0.5% to 1.2% a$^{-1}$ in the 1960–1990 and 1990–2011/12 periods, respectively (Table 4). The observed acceleration of glacier shrinkage is consistent with that reported for other regions of the Tien Shan [10,11,16]. Within the C-IRB region, the Kunes basin exhibited the highest (41%) loss of glacier area, which is surpassed only by the Khorgos basin (42%) (Table 8). The Kuksu basin, where glaciers are positioned at higher elevations, by contrast, exhibited one of the lowest losses of 25%, comparable with the Kax basin (27%).

In this study, we assessed changes in the extent of glaciers originally documented in the FCGI. However, our reassessment of the FCGI results for the Kuksu and Kunes basins revealed an underestimation of glacier extent by FCGI. In these two basins alone, 56 glaciers were not accounted for. Although their area constitutes about 1% of the glacier area as in the 1960s, other new inventories revealed that as late as in 2011/12, a number of glaciers with the total area more than 25 $km^2$ were mapped in other catchments of the C-IRB region, which were not documented in the original survey [40].

The data on glacier areas, together with the data on DJFs for snow and ice and partitioning of the total glacier runoff between the snow and ice components as measured at the Tuyuksu glacier, were used to evaluate the contribution of runoff due to ice melt and total runoff from the glacierized surfaces to river runoff. These contributions are poorly quantified in Central Asia [2] and, despite uncertainty associated with the methods of assessment, they provide an insight in water balance in C-IRB.

To date, there are no statistically significant trends in total river runoff in summer at any of four gauging sites in the C-IRB, although there are statistically significant negative trends at the Jiefangdaqiao site and the Qiedeke site in June and August, respectively. An increase in the cold-season discharge of the Ile was observed at the Yamadu station. These results are consistent with those published for other regions of the Tien Shan [29,31].

Both the PDD and the temperature-index methods show reductions in glacier runoff due to the melt of ice, and due to the combined melt of ice and snow. There is, however, a considerable discrepancy in the absolute values of runoff calculated by both methods, with the PDD method providing higher estimations in the Qiedeke basin (Figure 11). The total glacier runoff values, estimated using Krenke-Khodakov formula (Equation (2)), show that total glacier runoff accounts for, on average, 27% of the Qiedeke River, exceeding 60% in the very hot and dry years in the 1970s (Figure 12). The higher runoff values generated by the PDD method appear to provide unrealistically high values of the runoff due to ice melt in comparison with the total Qiedeke River runoff. The ablation measurements at the Tuyuksu glacier were conducted at approximately the same elevations (3480 and 3800 m) as the elevation of glacier tongue in the Qiedeke basin where they descend to 3300 m. However, the Qiedeke basin is characterized by lower humidity and, possibly, different importance of energy balance components, all of which can affect DDFs [60], leading to a poor performance of the PDD method. A more detailed assessment of PDD for snow and ice, and energy balance components and weather conditions, driving PDD at the Tuyuksu glacier, is required and will be performed in the future using data from the Automatic Weather Stations (AWS) installed on the Tuyuksu in 2015.

Although the temperature-index method was initially designed to calculate runoff for glaciers in the state of equilibrium, rather than under the conditions of rapid glacier retreat [64], there is a close agreement between the share of total glacier runoff in the total Ile River runoff at the Yamadu station, estimated by the temperature-index (17%) and ice volume reduction (18.5%) methods. Figure 13 provides a comparison of the annual Ile runoff at the Yamada station and total glacier runoff derived by the two methods. While the total annual river runoff has increased in the last two decades, in line with positive anomalies in precipitation (Figures 9 and 10), glacier runoff has been changing, in line with a decline of the glacier area driven by increasing JJA temperature (Table 8, Figure 9).

It should be noted that the uncertainty of the presented calculations of glacier runoff is high and is contributed to (i) the use of an empirical formula [64]; (ii) transfer of DDFs and partitioning of runoff from northern to eastern Tien Shan, despite the strong spatial variability characterizing DDFs [59,61]; (iii) use of the snow-ice runoff partitioning, which although changed from that obtained for the period of glacier stability [70], is applied uniformly to the 1963–2011 period; and (iv) the use of empirical volume-area scaling which, although known to accurately estimate the aggregate volume of a large number of glaciers, does not vary with time despite the strong wastage of glacier [65]. In the future, it will, therefore, be important to use and compare several different approaches, such as modeling and isotopic analysis.

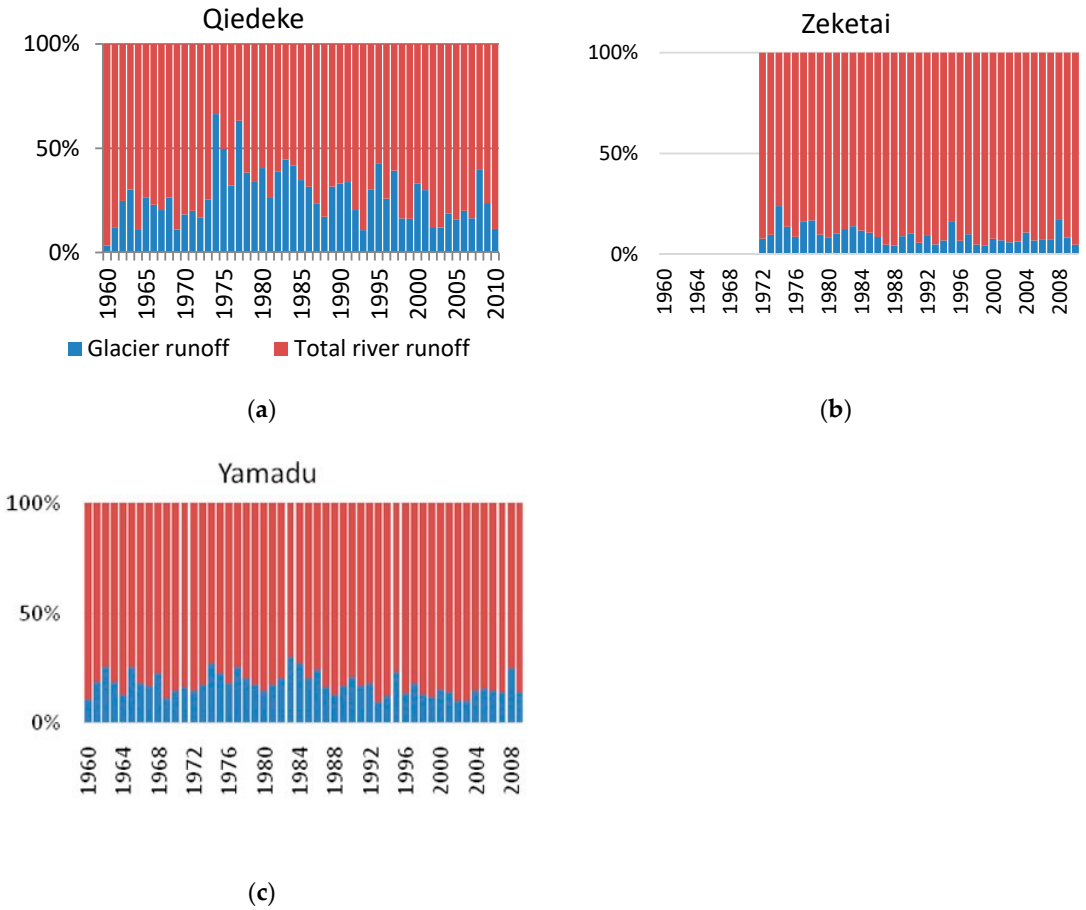


**Figure 12.** The share of the total glacier runoff in June-July-August (JJA) river runoff at Qiedeke (**a**), Zeketai (**b**) and Yamadu (**c**) stations.

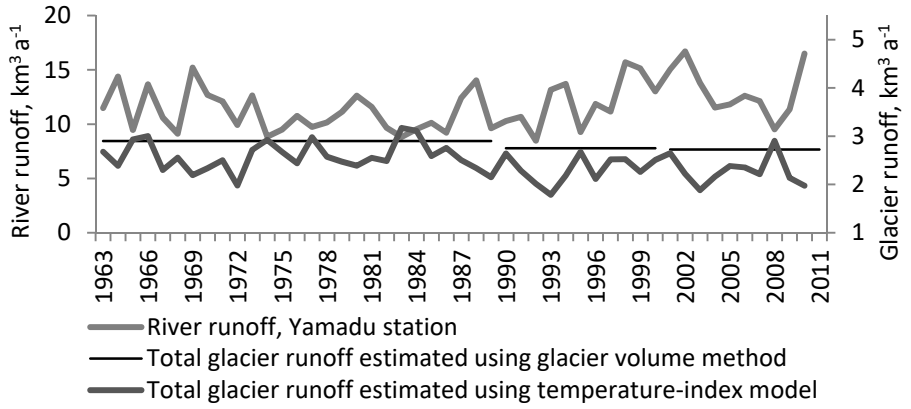


**Figure 13.** Change in the measured annual runoff of the Ile at the Yamadu station, total glacier runoff and runoff due to the melt of multiyear ice.

## 6. Conclusions

The main conclusions of this study are as follows:

1. In the Kuksu, Kunes, and Qiedeke basins of the C-IRB region, glaciers lost 191.3 km$^2$ or 36.9% of their initial area between the 1960s and 2010s;
2. Glacier wastage intensified from 0.5% to 1.2% a$^{-1}$ in the 1962/63–1990/93 and 1990/93–2012 periods, respectively;

3. There were no statistically significant trends in the streamflow of the Ile and its tributaries during the warm season to date, although negative trends were registered in the Qiedeke streamflow in August and, more recently, in the Tekes flow at Jiefangdaqiao in June;
4. Positive trends were registered in the Tekes flow at Jiefangdaqiao in winter and in the Ile flow at Yamadu in autumn, winter, and early spring, in line with similar trends observed in other regions of the Tien Shan; and
5. The estimations of total glacier runoff and runoff formed through the loss of multiyear ice in the Ile basin showed a reduction in both absolute values and its share in total river runoff since the 1980s in contrast to total river runoff.

**Author Contributions:** L.K., I.S. and M.S. designed the study. I.S. developed the theory. L.K. and I.S. collected the data and performed the analysis. L.K. and M.S. wrote the manuscript. B.L. supervised the manuscript.

**Funding:** This research was funded by Ministry of Education and Science of the Republic of Kazakhstan, grant number № ГФ AP05133077.

**Conflicts of Interest:** The authors declare no conflict of interest.

## References

1. Sorg, A.; Bolch, T.; Stoffel, M.; Solomina, O.; Beniston, M. Climate change impacts on glaciers and runoff in Tien Shan (Central Asia). *Nat. Clim. Chang.* **2012**, *2*, 725–731. [CrossRef]
2. Unger-Shayesteh, K.; Vorogushyn, S.; Farinotti, D.; Gafurov, A.; Duethmanna, D.; Mandychevc, A.; Merza, B. What do we know about past changes in the water cycle of Central Asian headwaters? A review. *Glob. Planet. Chang.* **2013**, *110*, 4–25. [CrossRef]
3. Groisman, P.; Shugat, H.; Kicklinghter, D.; Henerby, G.; Tchebakova, N.; Maksyutov, S.; Monier, E.; Gutman, G.; Gulev, S.; Qi, J.; et al. Northern Eurasia Future Initiative (NEFI): Facing the challenges and pathways of global change in the twenty-first century. *Prog. Earth Planet. Sci.* **2017**, *4*, 41. [CrossRef]
4. Shchetinnikov, S.A. *The Morphology and Regime of Pamir-Alai Glaciers*; Central Asia Hydro-Meteorological Institute: Tashken, Uzbekistan, 1998; p. 219. (In Russian)
5. Aizen, V.B.; Aizen, E.M.; Surazakov, A.B.; Kuzmichenok, V. Assessment of Glacial Area and Volume Change in Tien Shan (Central Asia) During the Last 150 years Using Geodetic, Aerial Photo, ASTER and SRTM Data. *Ann. Glaciol.* **2006**, *43*, 202–213. [CrossRef]
6. Li, B.; Zhu, A.X.; Zhang, Y.; Pei, T.; Qin, C.; Zhou, C. Glacier change over the past four decades in the middle Chinese Tien Shan. *J. Glaciol.* **2006**, *52*, 425–432. [CrossRef]
7. Shangguan, D.; Liu, S.; Ding, Y.; Ding, L.; Xu, J.; Li, J. Glacier changes during the last forty years in the Tarim Interior River basin, northwest China. *Prog. Nat. Sci.* **2006**, *19*, 727–732. [CrossRef]
8. Shi, Y. *Concise Glacier Inventory of China*; Popular Science Press: Shanghai, China, 2008; pp. 0–205.
9. Kotlyakov, V.; Severskiy, I. Glaciers of central Asia: Current situation, changes and possible impact on water resources. In *Assessment of Snow, Glacier and Water Resources in Asia*; Braun, L., Hagg, W., Severskiy, I., Young, G., Eds.; International Hydrological Program–Hydrology and Water Resources Programme: Koblenz, Germany, 2009; pp. 151–159.
10. Kutuzov, S.; Shahgedanova, M. Glacier retreat and climatic variability in the eastern Terskey-Alatoo, inner Tien Shan between the middle of the 19th century and beginning of the 21st century. *Global Planet. Chang.* **2009**, *69*, 59–70. [CrossRef]
11. Narama, C.; Kääb, A.; Duishonakunov, M.; Abdrakhmanov, K. Spatial variability of recent glacier area changes in the Tien Shan Mountains, Central Asia, using Corona (~1970), Landsat (~2000), and ALOS (~2007) satellite data. *Global Planet. Chang.* **2010**, *71*, 42–54. [CrossRef]
12. Wang, L.; Li, Z.; Wang, F.; Edwards, R. Glacier shrinkage in the Ebinur lake basin, Tien Shan, China, during the past 40 years. *J. Glaciol.* **2014**, *60*, 245–254. [CrossRef]
13. Farinotti, D.; Longuevergne, L.; Moholdt, G.; Duethmann, D.; Molg, T.; Bolch, T.; Vorogushin, S.; Guntner, A. Substantial glacier mass loss in the Tien Shan over the past 50 years. *Nat. Geosci.* **2015**, *8*, 716–722. [CrossRef]
14. Pieczonka, T.; Bolch, T. Region-wide glacier mass budgets and area changes for the Central Tien Shan between 1975 and 1999 using Hexagon KH-9 imagery. *Global Planet. Chang.* **2015**, *128*, 1–13. [CrossRef]
15. Cogley, J.G. Glacier shrinkage across High Mountain Asia. *Ann. Glaciol.* **2016**, *57*, 41–49. [CrossRef]

16. Severskiy, I.; Vilesov, E.; Armstrong, R.; Kokarev, A.; Kogutenko, L.; Usmanova, Z.; Morozova, V.; Raup, H.B. Changes in glaciers of the Balkhash-Alakol basin, Central Asia, over recent decades. *Ann. Glaciol.* **2016**, *57*, 382–394. [CrossRef]
17. WGMS. *Global Glacier Change Bulletin No. 2 (2014–2015)*, Based on database version; Zemp, M., Nussbaumer, S.U., GärtnerRoer, I., Huber, J., Machguth, H., Paul, F., Hoelzle, M., Eds.; ICSU(WDS)/IUGG(IACS)/UNEP/UNESCO/WMO, World Glacier Monitoring Service: Zurich, Switzerland, 2015; p. 244. [CrossRef]
18. Cao, M.S. Detection of abrupt changes in glacier mass balance in the Tien Shan Mountains. *J. Glaciol.* **1998**, *44*, 352–358. [CrossRef]
19. Vilesov, E.; Uvarov, V. *Evolution of the Recent Glaciation in the Zailyskiy Alatau in the 20th Century*; Kazakh State University: Almaty, Kazakhstan, 2001; pp. 0–252. (In Russian)
20. Severskiy, I.V.; Kokarev, A.L.; Severskiy, S.I.; Tokmagambetov, T.; Shesterova, I.; Shagalova, L. *Contemporary and Prognostic Changes of Glaciation in Balkhash Lake Basin*; VAC Publishing House: Almaty, Kazakhstan, 2006; p. 68.
21. Aizen, V.B.; Aizen, E.M.; Kuzmichenok, V.A. Glaciers and hydrological changes in the Tien Shan: Simulation and prediction. *Environ. Res. Lett.* **2007**, *2*, 045019. [CrossRef]
22. Bolch, T. Climate change and glacier retreat in northern Tien Shan (Kazakhstan/Kyrgyzstan) using remote sensing data. *Global Planet. Chang.* **2007**, *56*, 1–12. [CrossRef]
23. Yao, T.; Wang, Y.; Liu, S.; Pu, J.; Shen, Y.; Lu, A. Recent glacial retreat in the Chinese part of High Asia and its impact on water resources of Northwest China. In *Assessment of Snow, Glacier and Water Resources in Asia*; Braun, L., Hagg, W., Severskiy, I., Young, G., Eds.; International Hydrological Program–Hydrology and Water Resources Programme: Koblenz, Germany, 2009; pp. 26–35.
24. Barandun, M.; Huss, M.; Usubaliev, R.; Azisov, E.; Berthier, E.; Kääb, A.; Bolch, T.; Hoelzle, M. Multi-decadal mass balance series of three Kyrgyz glaciers inferred from modelling constrained with repeated snow line observations. *Cryosphere* **2018**, *12*, 1899–1919. [CrossRef]
25. Osmonov, A.; Bolch, T.; Xi, C.; Kurban, A.; Guo, W. Glacier characteristics and changes in the Sary-Jaz River Basin (Central Tien Shan, Kyrgyzstan)—1990–2010. *Remote Sens. Lett.* **2013**, *4*, 725–734. [CrossRef]
26. Niederer, P.; Bilenko, V.; Ershove, N.; Hurni, H.; Yerokin, S.; Maselli, D. Tracing glacier wastage in the Northern Tien Shan (Kyrgyzstan/Central Asia) over the last 40 years. *Clim. Chang.* **2008**, *86*, 227–234. [CrossRef]
27. Wang, S.; Zhang, M.; Li, Z.; Wang, F.; Li, H.; Li, Y.; Huang, X. Glacier area variation and climate change in the Chinese Tianshan Mountains since 1960. *J. Geogr. Sci.* **2011**, *21*, 263–273. [CrossRef]
28. Severskiy, I.V. Current and projected changes of glaciation in Central Asia and their probable impact on water resources. In *Assessment of Snow, Glacier and Water Resources in Asia*; UNESCO-IH and German IHP/HWRP National Committee: Koblenz, Germany, 2009; pp. 99–111.
29. Kriegel, D.C.; Mayer, W.; Hagg, S.; Vorogushin, S.; Duethmann, D.; Gafurov, A.; Farinotti, D. Changes in glacierisation, climate and runoff in the second half of the 20th century in the Naryn basin, Central Asia. *Global Planet. Chang.* **2013**, *110*, 51–61. [CrossRef]
30. Duethmann, D.; Menz, C.; Jiang, T.; Vorogushin, S. Projections for headwater catchments of the Tarim River reveal glacier retreat and decreasing surface water availability but uncertainties are large. *Environ. Res. Lett.* **2016**, *11*, 054024. [CrossRef]
31. Shahgedanova, M.; Afzal, M.; Severskiy, I.; Usmanova, Z.; Saidaliyeva, Z.; Kapitsa, V.; Kasatkin, N.; Dolgikh, S. Changes in the mountain river discharge in the northern Tien Shan since the mid-20th Century: Results from the analysis of a homogeneous daily streamflow data set from seven catchments. *J. Hydrol.* **2018**, *564*, 1133–1152. [CrossRef]
32. Hagg, W.; Hoelzle, M.; Wagner, S.; Mayr, E.; Klose, Z. Glacier and runoff changes in the Rukhk catchment, upper Amu-Darya basin until 2050. *Global Planet. Chang.* **2013**, *110*, 62–73. [CrossRef]
33. Ma, C.; Sun, L.; Liu, S.; Shao, M.; Luo, Y. Impact of climate change on the streamflow in the glacierized Chu River Basin, Central Asia. *J. Arid Land* **2015**, *7*, 501–513. [CrossRef]
34. Kraaijenbrink, P.D.A.; Bierkens, M.F.P.; Lutz, A.F.; Immerzeel, W. Impact of a global temperature rise of 1.5 degrees Celsius on Asia's glaciers. *Nature* **2017**, *549*, 257. [CrossRef]
35. Zhupankhan, A.; Tussupova, K.; Berndtsson, R. Could changing power relationships lead to better water sharing in Central Asia? *Water* **2017**, *9*, 139. [CrossRef]

36. Kezer, K.; Matsuyama, H. Decrease of river runoff in the Lake Balkhash basin in Central Asia. *Hydrol. Process.* **2006**, *20*, 1407–1423. [CrossRef]
37. Yapiyev, V.; Sagintayev, Z.; Verhoef, A.; Kassymbekova, A.; Baigaliyeva, M.; Zhumabayev, D.; Abudanash, D.; Ongdas, N.; Jumassultanova, S. The changing water cycle: Burabay National Nature Park, Northern Kazakhstan. *Water* **2017**, *4*, e1227. [CrossRef]
38. Ding, L.; Xie, W.; Liu, C.; Wang, C.; Wang, Z. *Glacier Inventory of China III. Tienshan Mountains (Ile River Drainage Basin)*; Science Press, Academia Sinica, Lanzhou Institute of Glaciology and Geocryology, Chinese Academy of Sciences: Beijing, China, 1986. (In Chinese)
39. Guo, W.; Liu, S.; Xu, J.; Wu, L.; Shangguan, D.; Yao, X.; Wei, J.; Bao, W.; Yu, P.; Liu, Q.; et al. The second Chinese glacier inventory: Data, methods and results. *J. Glaciol.* **2015**, *61*, 357–372. [CrossRef]
40. Xu, J.; Liu, S.; Guo, W.; Zhang, Z.; Wei, J.; Feng, T. Glacial Area Changes in the Ili River Catchment (Northeastern Tian Shan) in Xinjiang, China, from the 1960s to 2009. *Adv. Meteorol.* **2015**, 12. [CrossRef]
41. CMWR (China's Ministry of Water Resources). *Evaluation of Chinese Water Resources*; Water Resources Publisher: Beijing, China, 1987; p. 194. (In Chinese)
42. Severskiy, I.V.; Xie, Z. *Snow Cover and Avalanches in Tien Shan Mountains*; VAC Publishing House: Almaty, Kazakhstan, 2000; p. 179.
43. Severskiy, I.; Blagoveshenskiy, V. *Estimation of Avalanches Hazards of Mountain Area*; Science: Almaty, Kazakhstan, 1983; p. 215. (In Russian)
44. Schroder, H.; Severskiy, I. *Water Resources in the Basin of the Ili River (Republic of Kazakhstan): Final Report*; Mensch and Buch Verlag: Berlin, Germany, 2004; p. 310.
45. Kendall, M.G. *Rank Correlation Methods*; Griffin: London, UK, 1975.
46. Jaiswal, R.K.; Lohani, A.K.; Tiwari, H.L. Statistical Analysis for Change Detection and Trend Assessment in Climatological Parameters. *Environ. Process.* **2015**, *2*, 729–749. [CrossRef]
47. GLOVIS. Available online: http://glovis.usgs.gov/ (accessed on 23 June 2019).
48. GLIMS: Global Land Ice Measurements from Space. Available online: http://www.glims.org/ (accessed on 23 June 2019).
49. Arendt, A.; Bliss, A.; Bolch, T.; Cogley, J.G.; Gardner, A.S.; Hagen, J.-O.; Hock, R.; Huss, M.; Kaser, G.; Kienholz, C.; et al. Randolph Glacier Inventory—A Dataset of Global Glacier Outlines: Version 4.0. In *Global Land Ice Measurements from Space*; Digital Media: Boulder, CO, USA, 2014.
50. Arendt, A.; Bliss, A.; Bolch, T.; Cogley, J.G.; Gardner, A.S.; Hagen, J.-O.; Hock, R.; Huss, M.; Kaser, G.; Kienholz, C.; et al. Randolph Glacier Inventory—A Dataset of Global Glacier Outlines: Version 5.0. In *Global Land Ice Measurements from Space*; Digital Media: Boulder, CO, USA, 2015.
51. Global Land Survey 2000. Available online: http://landsat.usgs.gov/GLS2000_Accuracy.php (accessed on 23 June 2019).
52. ASTER Global Digital Elevation Map. Available online: https://asterweb.jpl.nasa.gov/gdem.asp (accessed on 23 June 2019).
53. Kapitsa, V.; Shahgedanova, M.; Machguth, H.; Severskiy, I.; Medeu, A. Assessment of evolution and risks of glacier lake outbursts in the Djungarskiy Alatau, Central Asia, using Landsat imagery and glacier bed topography modelling. *Nat. Hazards Earth Syst. Sci.* **2017**, *17*, 1837–1856. [CrossRef]
54. Bolch, T.; Kamp, U. Glacier mapping in high mountains using DEMs, Landsat and ASTER data. *Grazer Schr. Geogr. Raumforsch.* **2006**, *41*, 13–24.
55. Paul, F.; Barry, R.G.; Cogley, J.G.; Frey, H.; Haeberli, W.; Ohmura, A.; Ommanney, C.S.L.; Raup, B.; Rivera, A.; Zemp, M. Recommendations for the compilation of glacier inventory data from digital sources. *Ann. Glaciol.* **2009**, *50*, 119–126. [CrossRef]
56. Kokarev, A.; Shesterova, I. Change of the glacier systems on the northern slope of Zailiyskiy Alatau for the second half of XX and the beginning of XXI centuries. *Ice Snow* **2011**, *4*, 39–46. (In Russian)
57. Bolch, T.; Menounos, B.; Wheate, R. Landsat-based inventory of glaciers in western Canada, 1985–2005. *Remote Sens. Environ.* **2010**, *114*, 127–137. [CrossRef]
58. Cogley, J.G.; Hock, R.; Rasmussen, L.A.; Arendt, A.A.; Bauder, A.; Braithwaite, R.J.; Jansson, P.; Kaser, G.; Möller, M.; Nicholson, L.; et al. *Glossary of Glacier Mass Balance and Related Terms*; IHP-VII Technical Documents in Hydrology No. 86, IACS Contribution No. 2; UNESCO-IHP: Paris, France, 2011.
59. Braithwaite, R. Temperature and precipitation climate at the equilibrium-line altitude of glaciers expressed by the degree-day factor for melting snow. *J. Glaciol.* **2008**, *54*, 437–444. [CrossRef]

60. Hock, R. Temperature Index Melt Modelling in Mountain Areas. *J. Hydrol.* **2003**, *282*, 104–115. [CrossRef]
61. Lang, H.; Braun, L. On the information content of air temperature in the context of snow melt estimation. In *Hydrology of Mountainous Areas, Proceedings of the Strbské Pleso Workshop, Czechoslovakia, Strbské Pleso 1 June 1988*; Molnar, L., Ed.; International Association of Hydrological Sciences Publication: Wallingford, UK, 1990; pp. 347–354.
62. Yatagai, A.O.; Arakawa, K.; Kamiguchi, H.; Kawamoto, H.; Nodzu, M.I.; Hamada, A. A 44-year daily gridded precipitation dataset for Asia based on a dense network of rain gauges. *SOLA* **2009**, *5*, 137–140. [CrossRef]
63. Yatagai, A.K.; Kamiguchi, O.; Arakawa, A.; Hamada, A.; Yasutomi, N.; Kitoh, A. APHRODITE: Constructing a Long-term Daily Gridded Precipitation Dataset for Asia based on a Dense Network of Rain Gauges. *Bull. Am. Meteorol. Soc.* **2012**. [CrossRef]
64. Krenke, A. *Mass Transfer in Glacial Systems in the USSR*; Gydrometeoizdat: Leningrad, Russia, 1982; p. 288. (In Russian)
65. Bahr, D.; Pfeffer, W.; Kaser, G. A review of volume-area scaling of glaciers. *Rev. Geophys.* **2014**, *53*, 95–140. [CrossRef] [PubMed]
66. Chen, J.; Ohmura, A. Estimation of Alpine glacier water resources and their change since the 1870s. Hydrology in mountainous regions. In *I–Hydrological Measurements; the Water Cycle, Proceedings of Two Lausanne Symposia, August 1990*; International Association of Hydrological Sciences Publication: Wallingford, UK, 1990; Volume 193, pp. 127–135.
67. Raper, S.C.; Braithwaite, R.J. Low sea level rise projections from mountain glaciers and icecaps under global warming. *Nature* **2006**, *439*, 311–313. [CrossRef] [PubMed]
68. Farinotti, D.; Huss, M.; Bauder, A.; Funk, M.; Truffer, M. A method to estimate ice volume and ice thickness distribution of alpine glaciers. *J. Glaciol.* **2009**, *55*, 422–430. [CrossRef]
69. Radic, V.; Hock, R. Regionally differentiated contribution of mountain glaciers and ice caps to future sea-level rise. *Nat. Geosci.* **2011**, *4*, 91–94. [CrossRef]
70. Sosedov, I. *Methods of Territorial Water Balance Generalizations in the Mountains*; Nauka: Almaty, Kazakhstan, 1976; p. 154. (In Russian)
71. Armstrong, R.L. *The Glaciers of the Hindu Kush-Himalayan Region: A Summary of the Science Regarding glacier Melt/Retreat in the Himalayanm, Hindu Kush, Karakorum, Pamir, and Tien Shan mountain ranges*; Technical Report; International Centre for Integrated Mountain Development (ICIMOD): Kathmandu, Nepal, 2010; pp. 0–16.
72. Kotlyakov, V. *Glaciologycal Dictionary*; Hydrometeoizdat: Leningra, Russia, 1984; p. 564. (In Rusian)
73. Kemmerikh, A.O. *Rol'lednikov v stoke rek Sredney Azii*; (The role of glaciers for river runoff in Central Asia), Materialy Glaciologicheskikh Issledovanii (Data of Glaciological Studies); Nauka Publisher: Moscow, Russia, 1972; Volume 20, pp. 82–94. (In Russian)
74. He, Y.; Pang, H.; Theakstone, W.; Zhang, D.; Lu, A.; Song, B.; Yuan, L.; Ning, B. Spatial and temporal variations of oxygen isotopes in snowpacks and glacial runoff in different types of glacial area in western China. *Ann. Glaciol.* **2006**, *43*, 269–274. [CrossRef]
75. Wang, N.; Zhang, S.; He, J.; Pu, J.; Wu, X.B.; Xi, J. Tracing the major source area of the mountainous runoff generation of the Heihe River in northwest China using stable isotope technique *Chin. Sci. Bull.* **2009**, *54*, 2751–2757. [CrossRef]
76. Oberhänsli, H.; Weise, S.; Stanichny, S. Oxygen and hydrogen isotopic water characteristics of the Aral Sea, Central Asia. *J. Mar. Syst.* **2009**, *76*, 310–321. [CrossRef]
77. Dahlke, H.E.; Lyon, S.W.; Jansson, P.; Karlin, T.; Rosqvist, G. Isotopic investigation of runoff generation in a glacierized catchment in northern Sweden. *Hydrol. Process.* **2016**, *28*, 1383–1398. [CrossRef]
78. Dyurgerov, M.B.; Liu, C.; Xie, Z. *Tien Shan Glaciers*; BINITI: Moscow, Russia, 1995; p. 233. (In Russian)
79. Glazirin, G.E. *Distribution and Regime of Mountain Glaciers*; Hydrometeoizdat: Leningrad, Russia, 1985; p. 180. (In Russian)
80. Makarevich, K.G.; Vilesov, E.N.; Golovkova, R.G.; Denisova, T.J.; Shabanov, P.F. *The Tuyuksu Glaciers (North Tien Shan)*; Gidrometeoizdat: Leningrad, Russia, 1984; p. 170. (In Russian)
81. Wang, P.; Li, Z.; Huai, B.; Wang, W.; Li, H.; Wang, L. Spatial variability of glacial changes and their effects on water resources in the Chinese Tianshan Mountains during the last five decades. *J. Arid Land* **2015**, *7*, 717–727. [CrossRef]
82. Vilesov, E.; Morozova, V.; Severskiy, I. *Glaciation Jungar (Zhetysu) Alatau: Past, Present, Future*; PH KazNU: Almaty, Kazakhstan, 2013; p. 244. (In Russian)

83. Kaldybaev, A.; Chen, Y.; Vilesov, E. Glacier change in the Karatal river basin, Zhetysu (Dzhungar) Alatau, Kazakhstan. *Ann. Glaciol.* **2016**, *57*, 11–19. [CrossRef]
84. Liu, S.; Su, Z.; Zhao, J.; Dong, D. *Chinese Glacier Illustrations*; Chinese Edition.; Popular Science Press: Shanghai, China, 2014; p. 150.